Electronic Supplementary Material (ESI) for Inorganic Chemistry Frontiers.

Novel Osmium(II)-Cymene Complexes Containing Curcumin and Bisdemethoxycurcumin ligands

Riccardo Pettinari,[a]* Fabio Marchetti,[b] Corrado Di Nicola,[b] Claudio Pettinari,[a] Massimiliano Cuccioloni,[c] Laura Bonfili,[c] Anna Maria Eleuteri,[c] Bruno Therrien,[d] Lucida Kate Batchelor,[e] Paul J. Dyson.[e]*

[a] School of Pharmacy, [b]School of Science and Technology, [c]School of Biosciences and Veterinary Medicine University of Camerino, via S. Agostino 1, 62032 Camerino MC, Italy, [d]Institute of Chemistry, University of Neuchatel, Avenue de Bellevaux 51, CH-2000 Neuchatel, Switzerland; [e]Institut des Sciences et Ingénierie Chimiques, École Polytechnique Fédérale de Lausanne (EPFL), 1015 Lausanne, Switzerland.

Supplementary Information

Table of contents

X-Ray data

Far-IR data

Relevant NMR spectra

Biological studies

Table S1 – Crystallographic data and structure refinement details for compound **1**.

	1
Chemical formula	$C_{31}H_{33}ClO_6Os$
Formula weight	727.22
Crystal system	Orthorhombic
Space group	*Pbca* (no. 61)
Crystal color and shape	Orange block
Crystal size	0.22 x 0.19 x 0.18
a (Å)	7.9750(3)
b (Å)	22.7119(11)
c (Å)	32.7398(14)
V (Å^3)	5930.1(4)
Z	8
T (K)	293(2)
D_c (g·cm^{-3})	1.629
μ (mm^{-1})	4.432
Scan range (°)	$1.79 < \theta < 29.28$
Unique reflections	7961
Observed refls [I>2σ(I)]	4001
R_{int}	0.1065
Final *R* indices [I>2σ(I)]*	0.0937, wR_2 0.2150
R indices (all data)	0.1779, wR_2 0.2565
Goodness-of-fit	1.029
Max, Min Δρ/e (Å^{-3})	4.927, - 2.094

Table S2 – Selected bond distances (Å) and angles (º) for compound **1**.

Distances (Å)	
Os-O1	2.092(9)
Os-O2	2.088(9)
Os-Cl	2.430(4)
C9-O1	1.293(16)
C11-O2	1.257(16)
C9-C10	1.359(19)
C10-C11	1.392(18)
Os-centroid	1.65

Angles (°)	
O1-Os-O2	87.0(4)
O1-Os-Cl	84.6(3)
O2-Os-Cl	85.7(3)

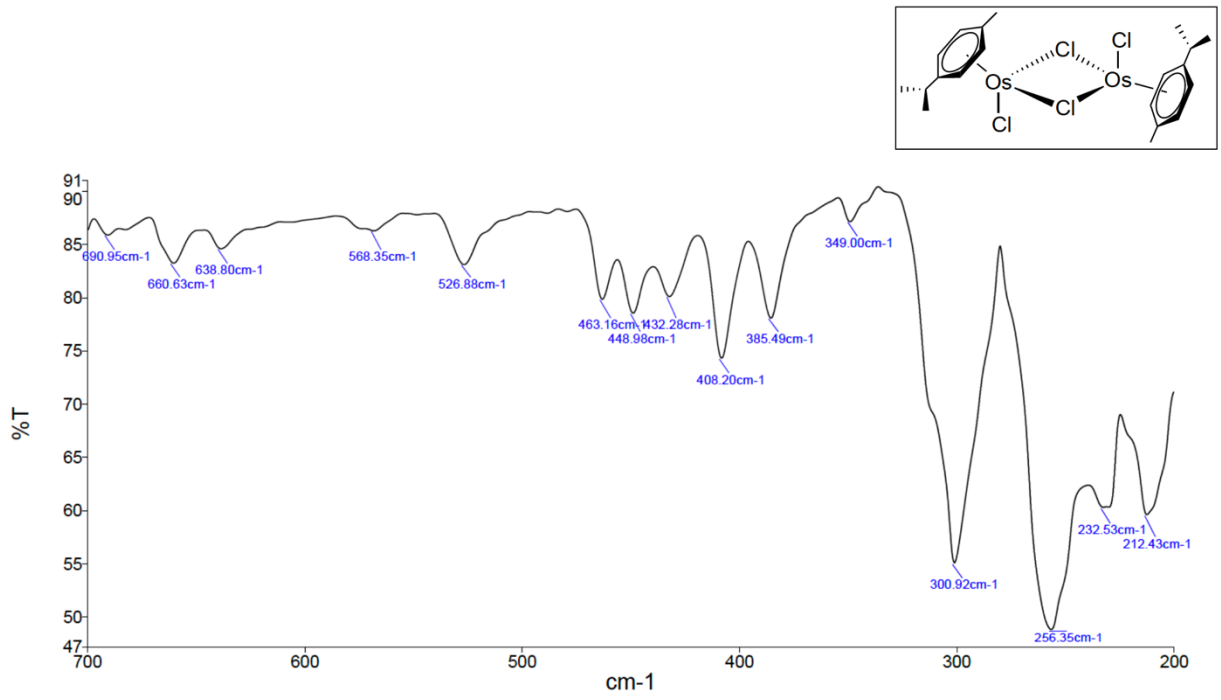

Figure S1. Far-IR of **[(*p*-cym)OsCl$_2$]**.

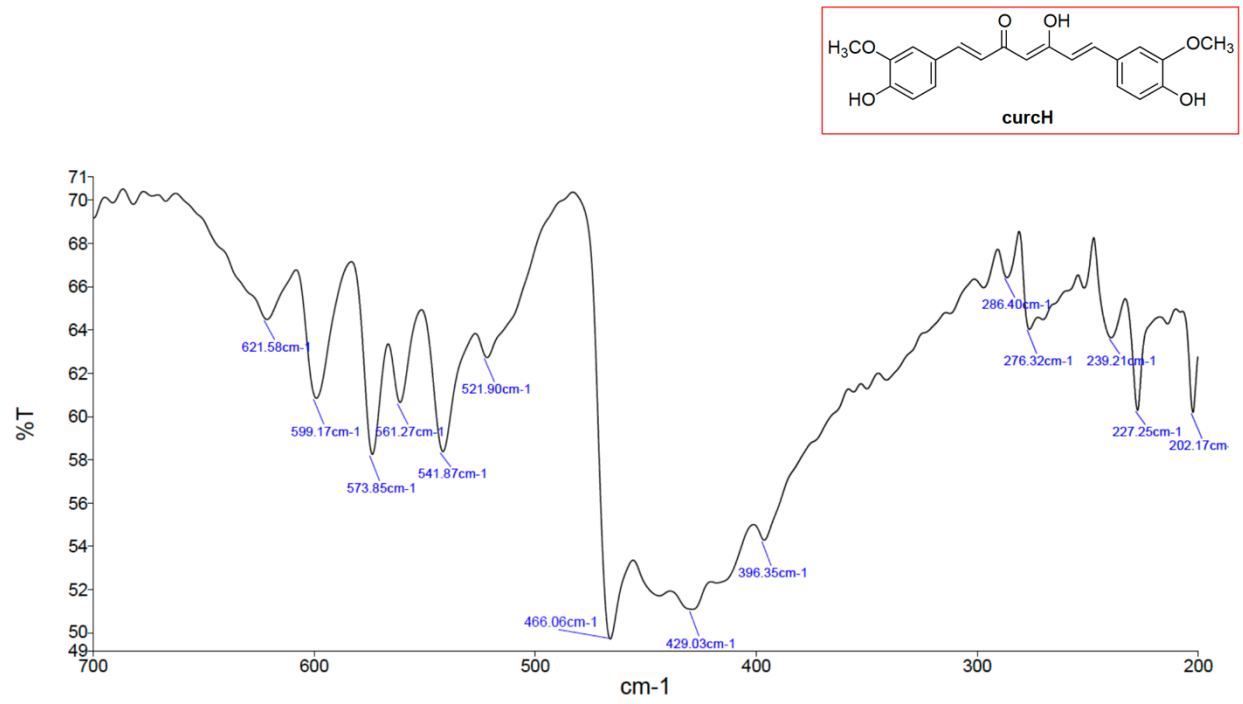

Figure S2. Far-IR of **curcH**.

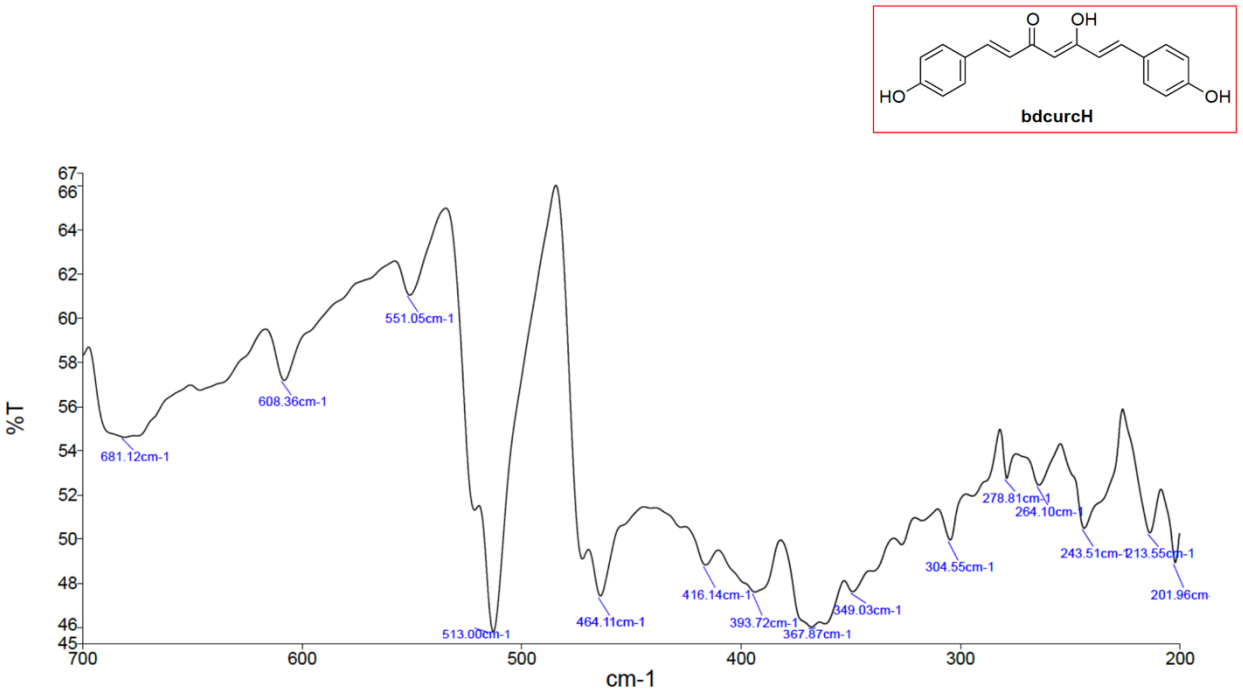

Figure S3. Far-IR of **bdcurcH**.

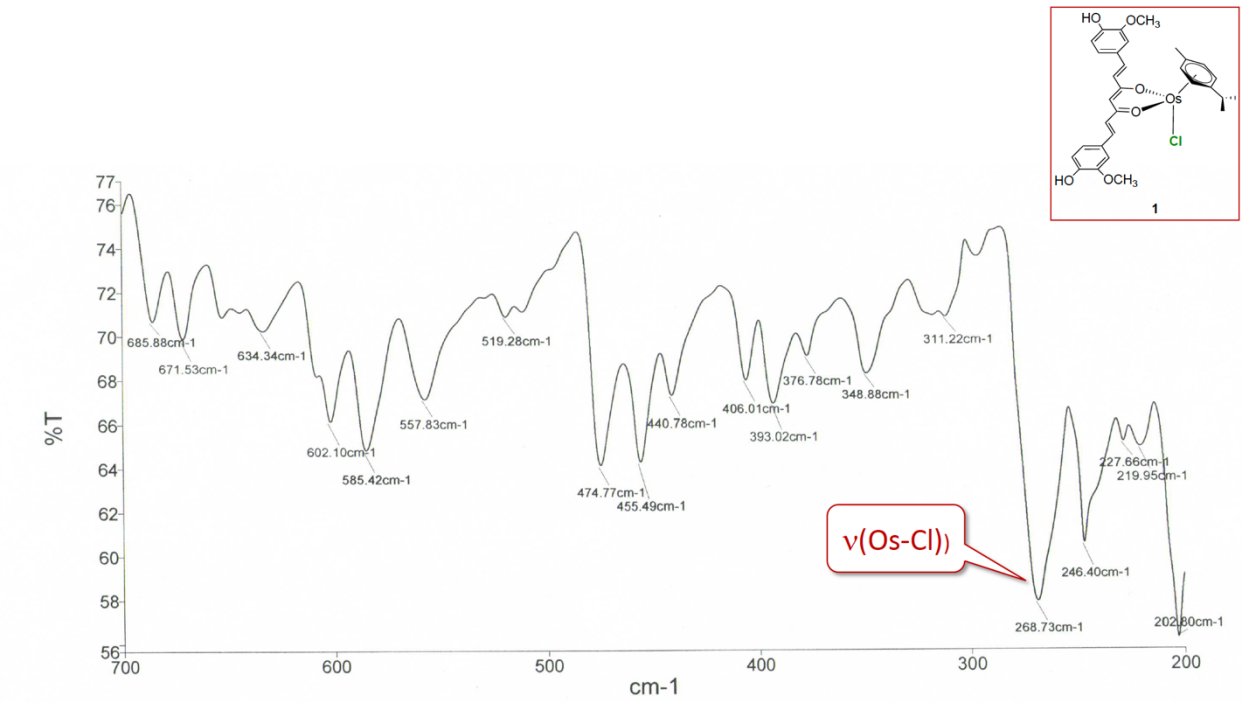

Figure S4. Far-IR of **1**.

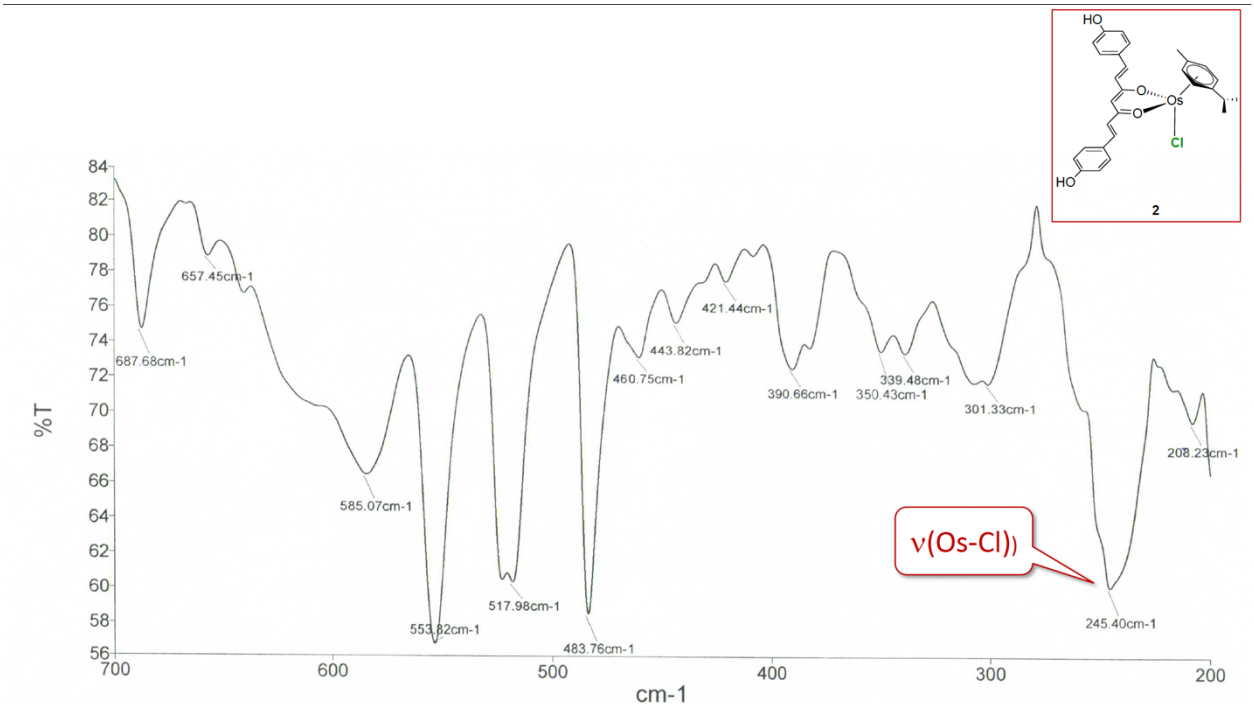

Figure S5. Far-IR of **2**.

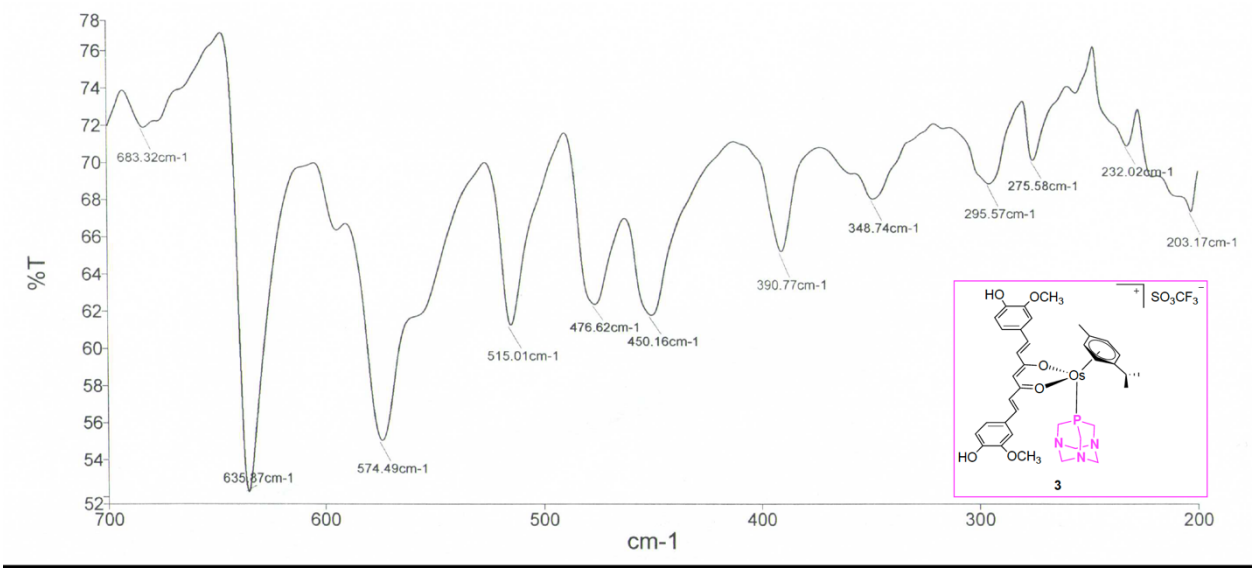

Figure S6. Far-IR of **3**.

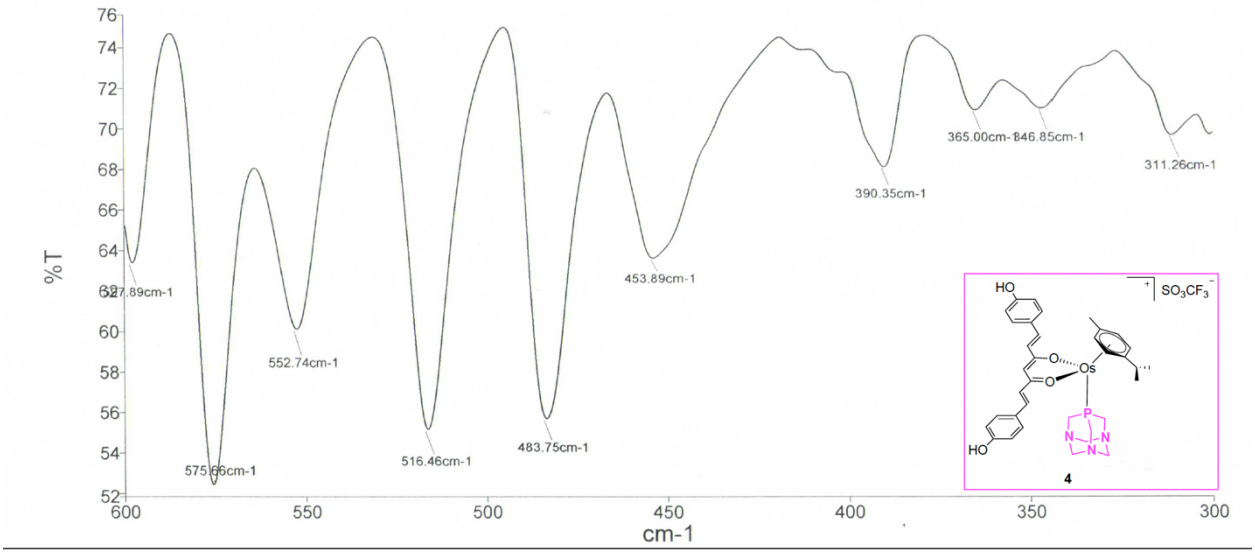

Figure S7. Far-IR of **4**.

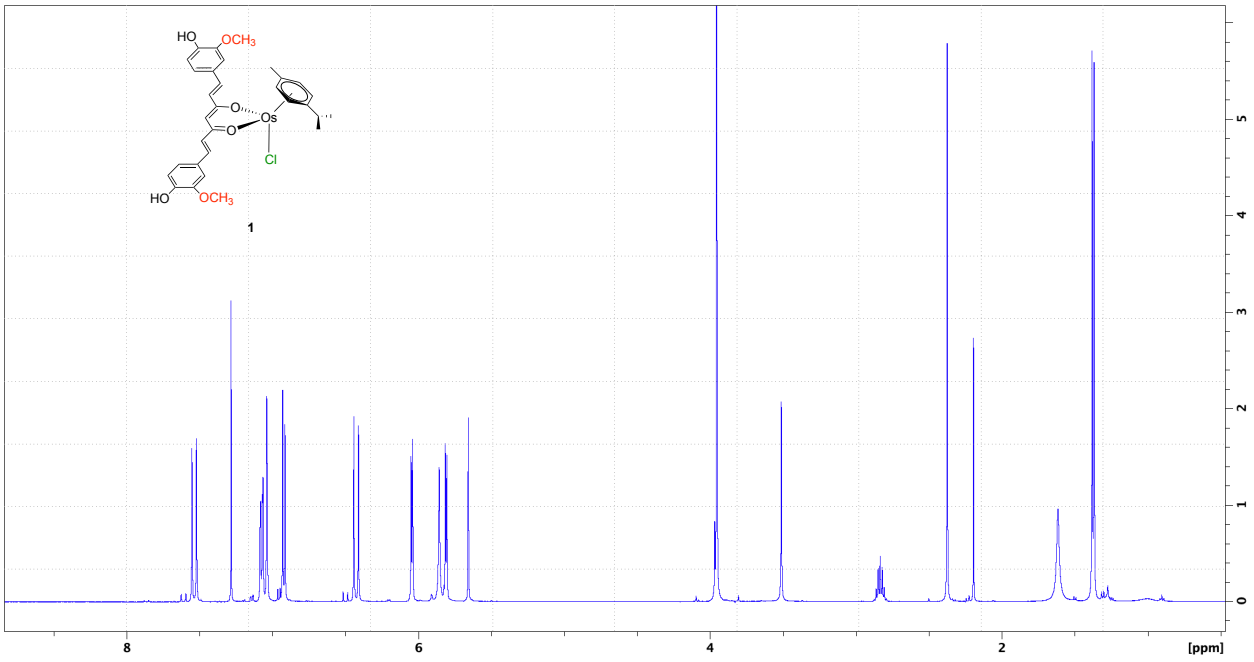

Figure S8. ^{1}H NMR spectrum in $CDCl_3$ at 298 K of **1**.

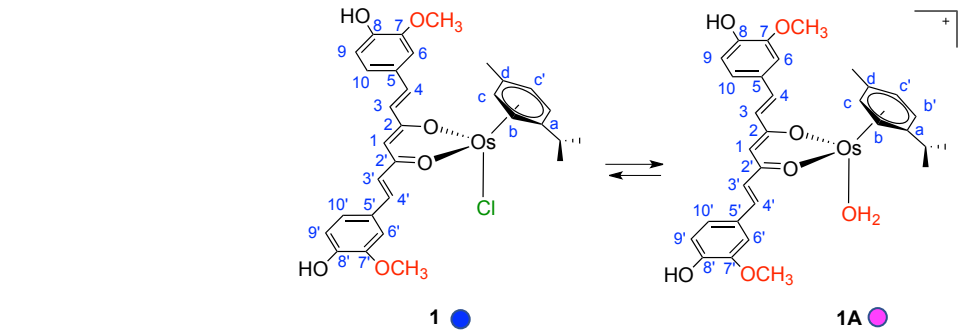

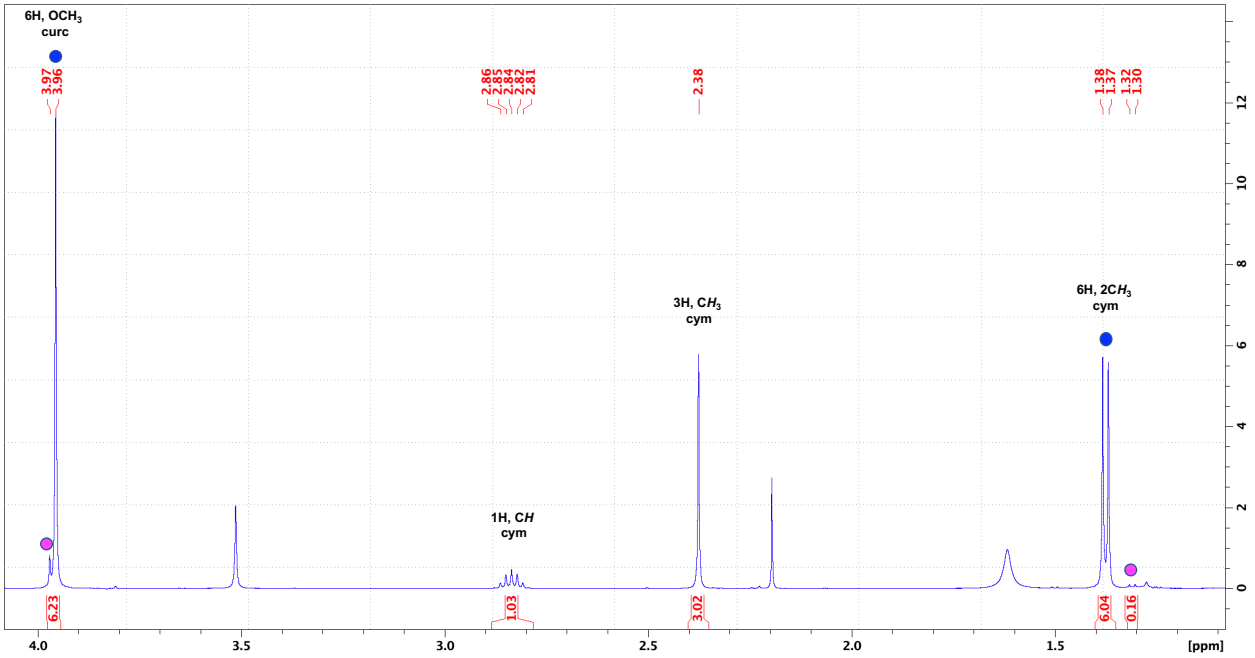

Figure S9. Magnification of ^{1}H NMR spectrum in $CDCl_3$ at 298 K of **1.**

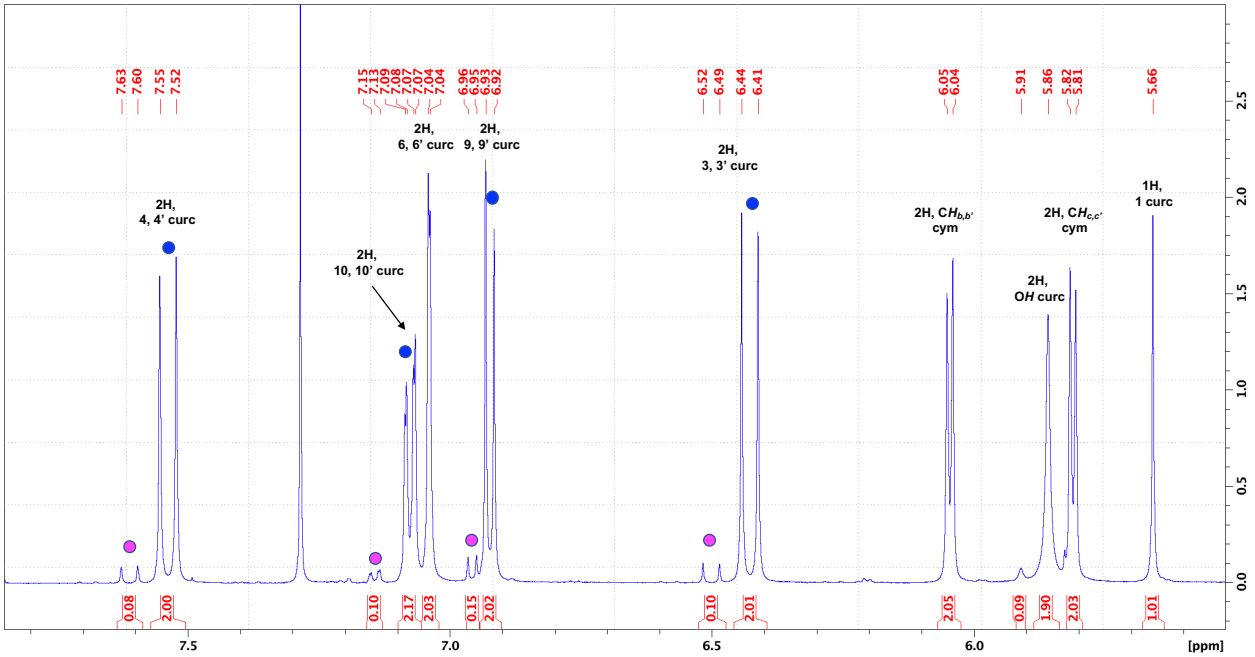

Figure S10. Magnification of ^{1}H NMR spectrum in $CDCl_3$ at 298 K of **1**.

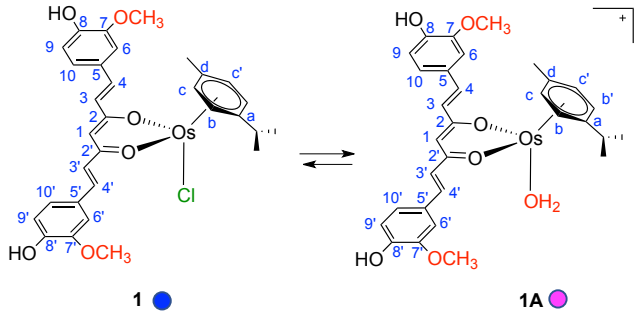

1D TopSPIN Multiplet Table

ID	Shift [ppm]	J [Hz]	M	Connection
1	7.6109	15.7541	2	J(1, 8)
2	7.5375	15.6041	2	J(2, 9)
3	7.1430	1.6004	2	J(3, 5)
		8.2021	2	J(3, 0)
4	7.0758	6.5017	2	J(4, 0)
5	7.0392	1.6004	2	J(5, 3)
6	6.9569	8.1021	2	J(6, 7)
7	6.9235	8.1521	2	J(7, 6)
8	6.5010	15.7541	2	J(8, 1)
9	6.4275	15.6041	2	J(9, 2)
10	6.0456	5.6015	2	J(10, 11)
11	5.8109	5.6015	2	J(11, 10)
12	2.8353	13.8536	2	J(12, 0)
13	1.3758	6.9518	2	J(13, 14)
14	1.3099	7.0018	2	J(14, 13)

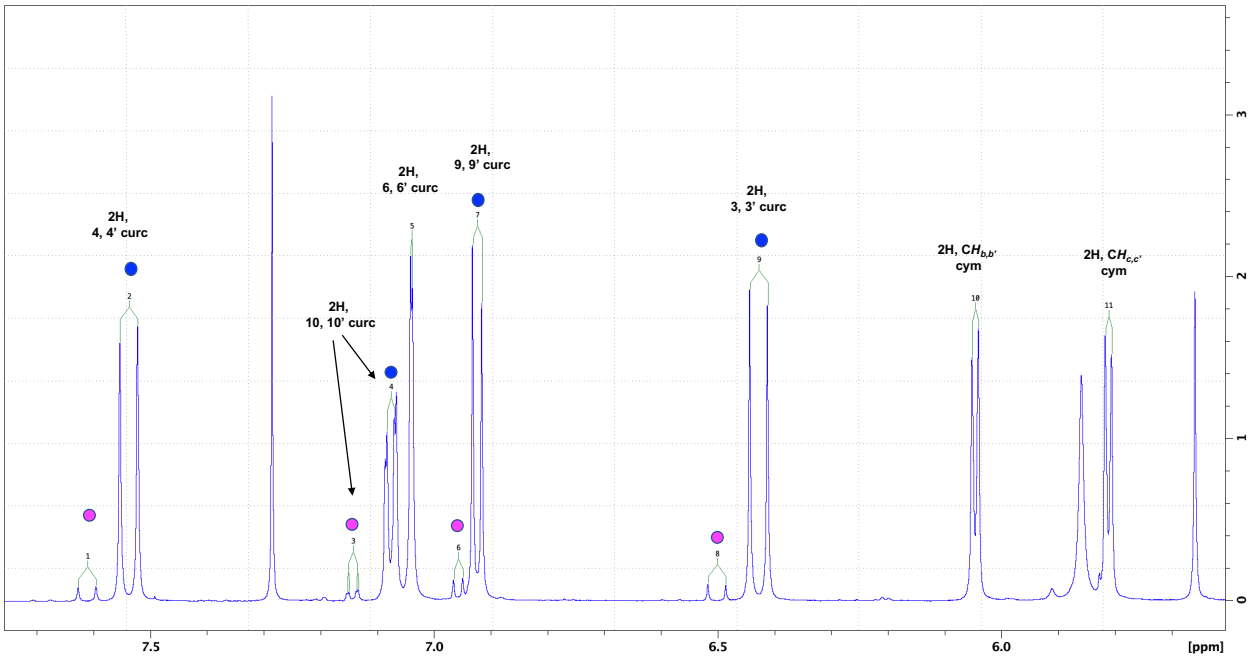

Figure S11. Magnification of ^{1}H NMR spectrum in $CDCl_3$ at 298 K of **1**.

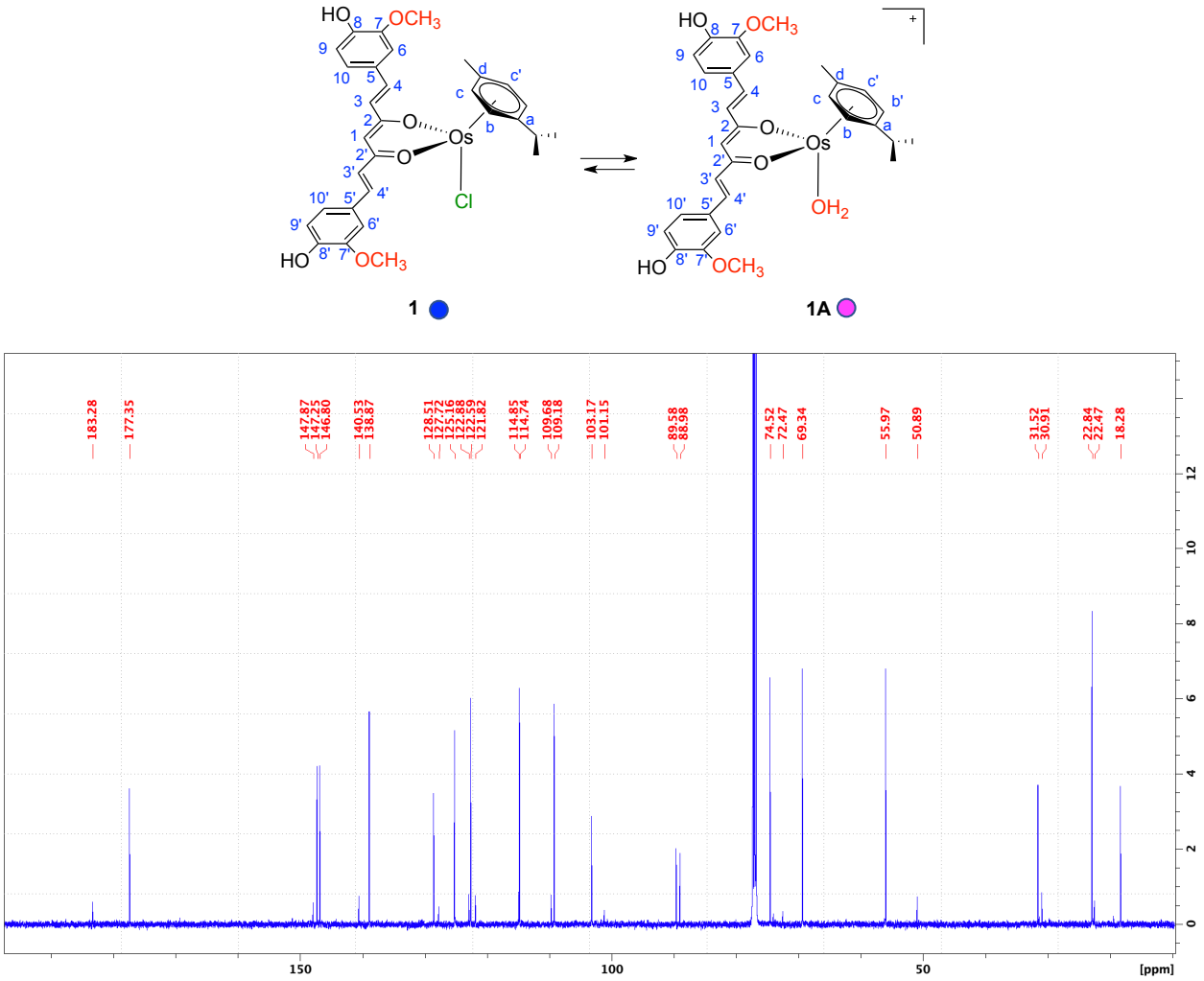

Figure S12. ^{13}C NMR spectrum in $CDCl_3$ at 298 K of **1**.

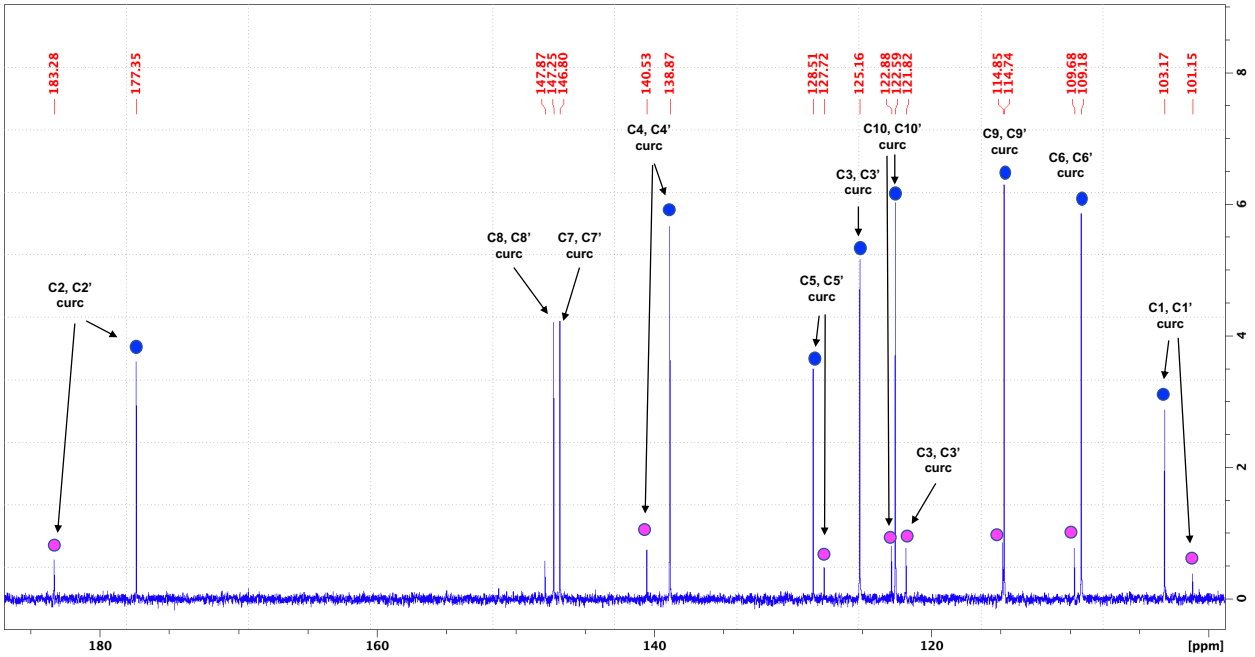

Figure S13. Magnification of ^{13}C NMR spectrum in $CDCl_3$ at 298 K of **1**.

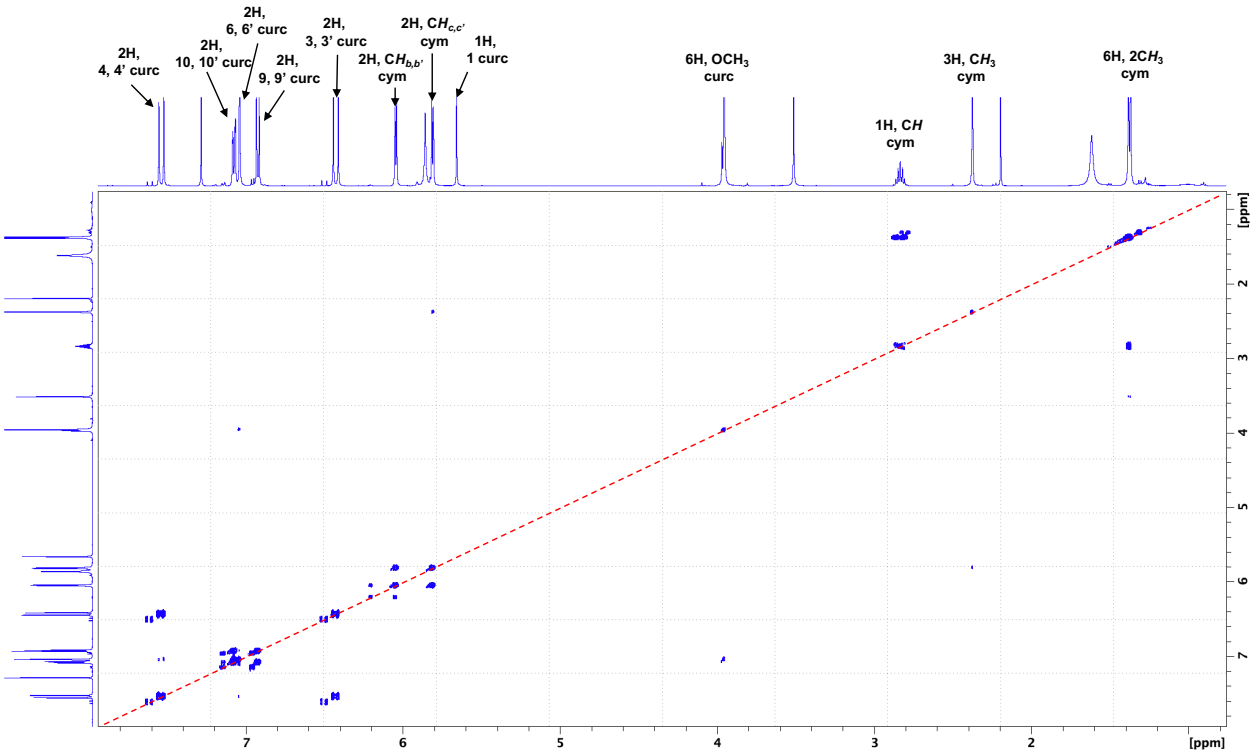

Figure S14. {^{1}H, ^{1}H}-COSY spectrum in $CDCl_3$ at 298 K of **1**.

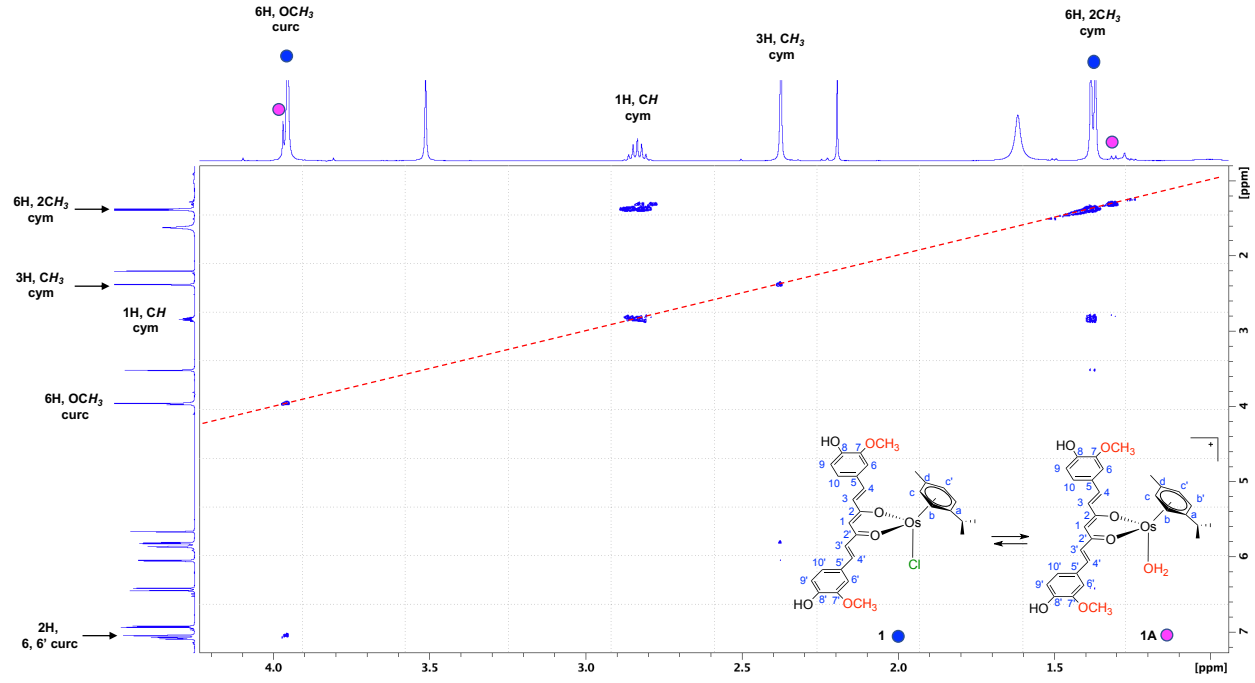

Figure S15. Magnification of {^{1}H, ^{1}H}-COSY spectrum in $CDCl_3$ at 298 K of **1**.

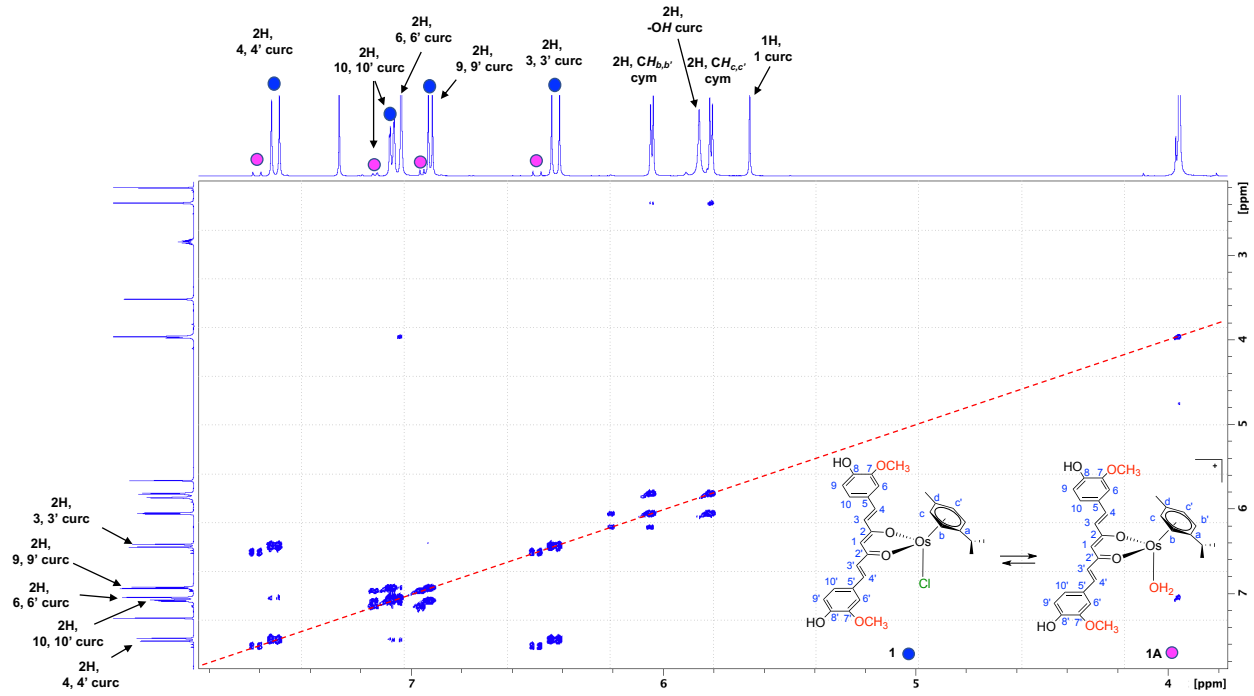

Figure S16. Magnification of {^{1}H, ^{1}H}-COSY spectrum in $CDCl_3$ at 298 K of **1**.

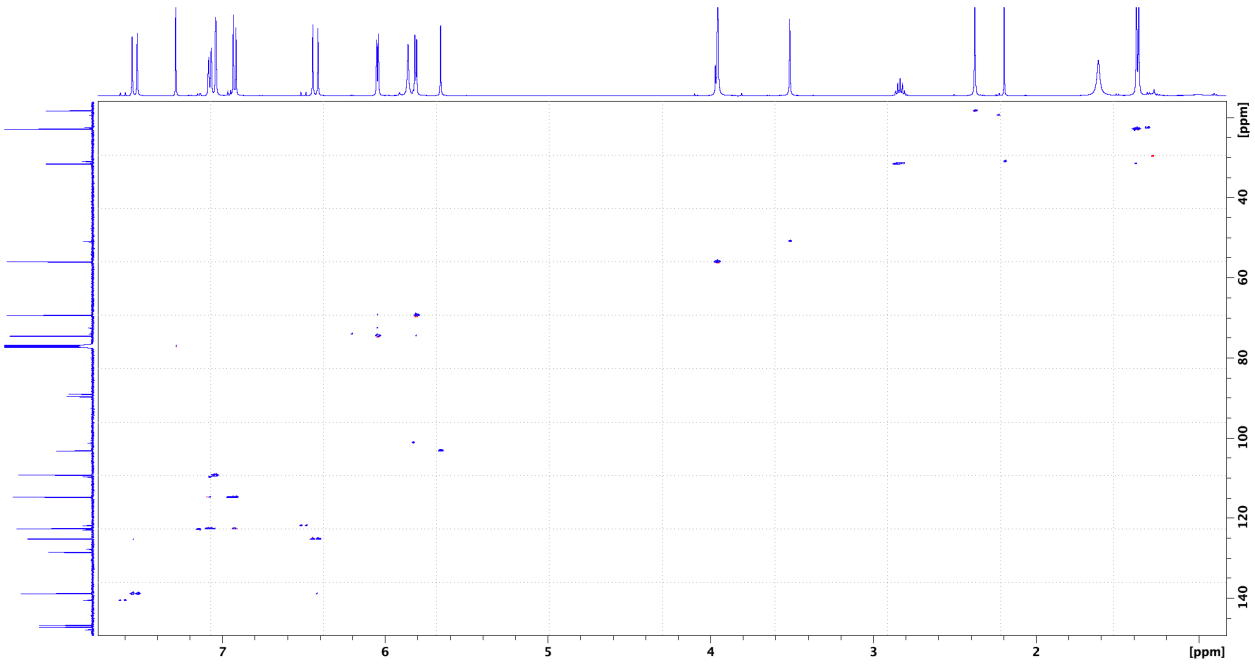

Figure S17. {^{1}H, ^{13}C}-HSQC spectrum in $CDCl_3$ at 298 K of **1**.

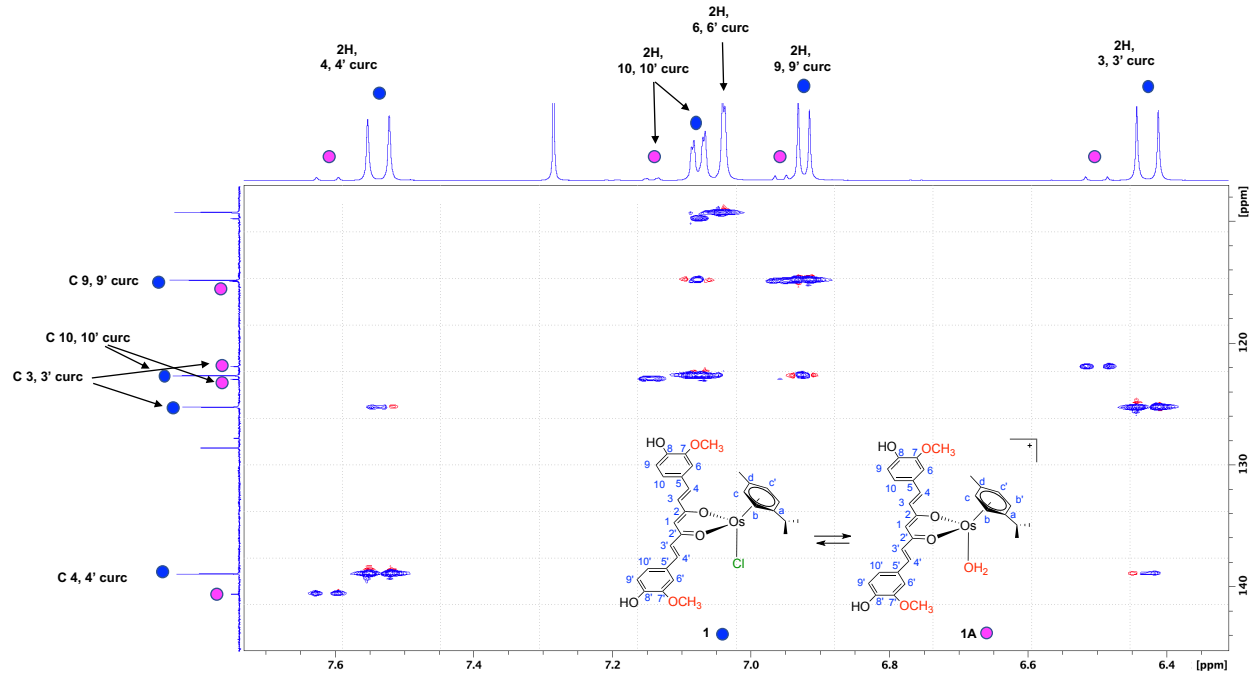

Figure S18. Magnification of {^{1}H, ^{13}C}-HSQC spectrum in $CDCl_3$ at 298 K of **1**.

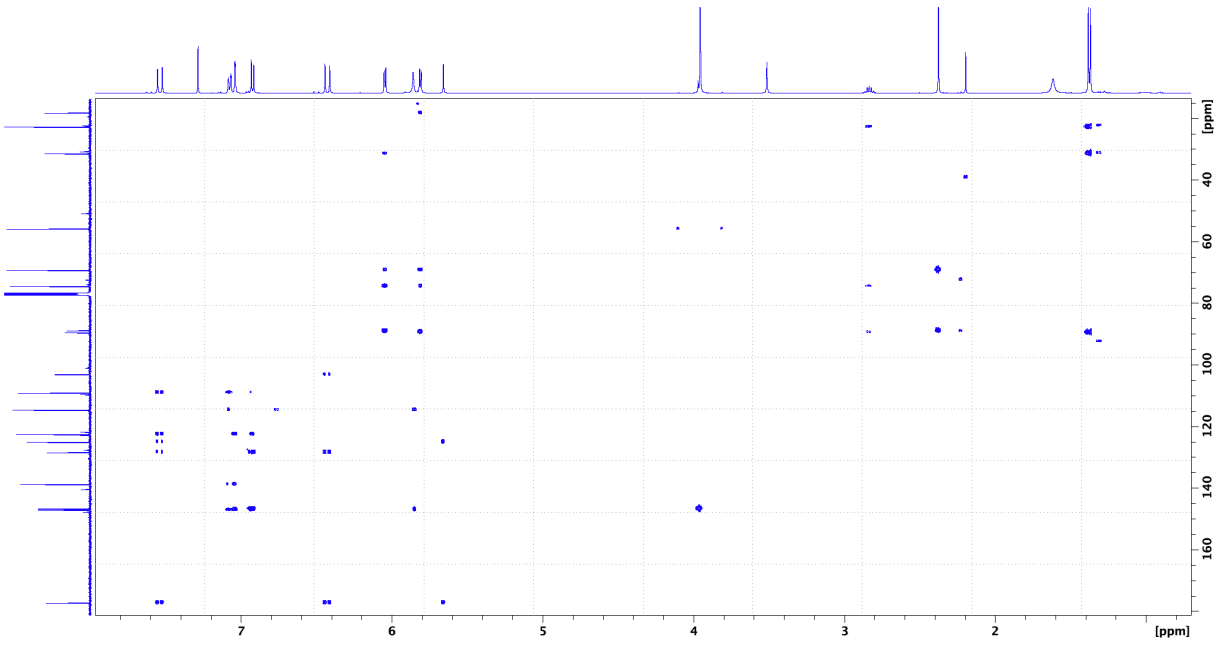

Figure S19. {^{1}H, ^{13}C}-HMBC spectrum in $CDCl_3$ at 298 K of **1**.

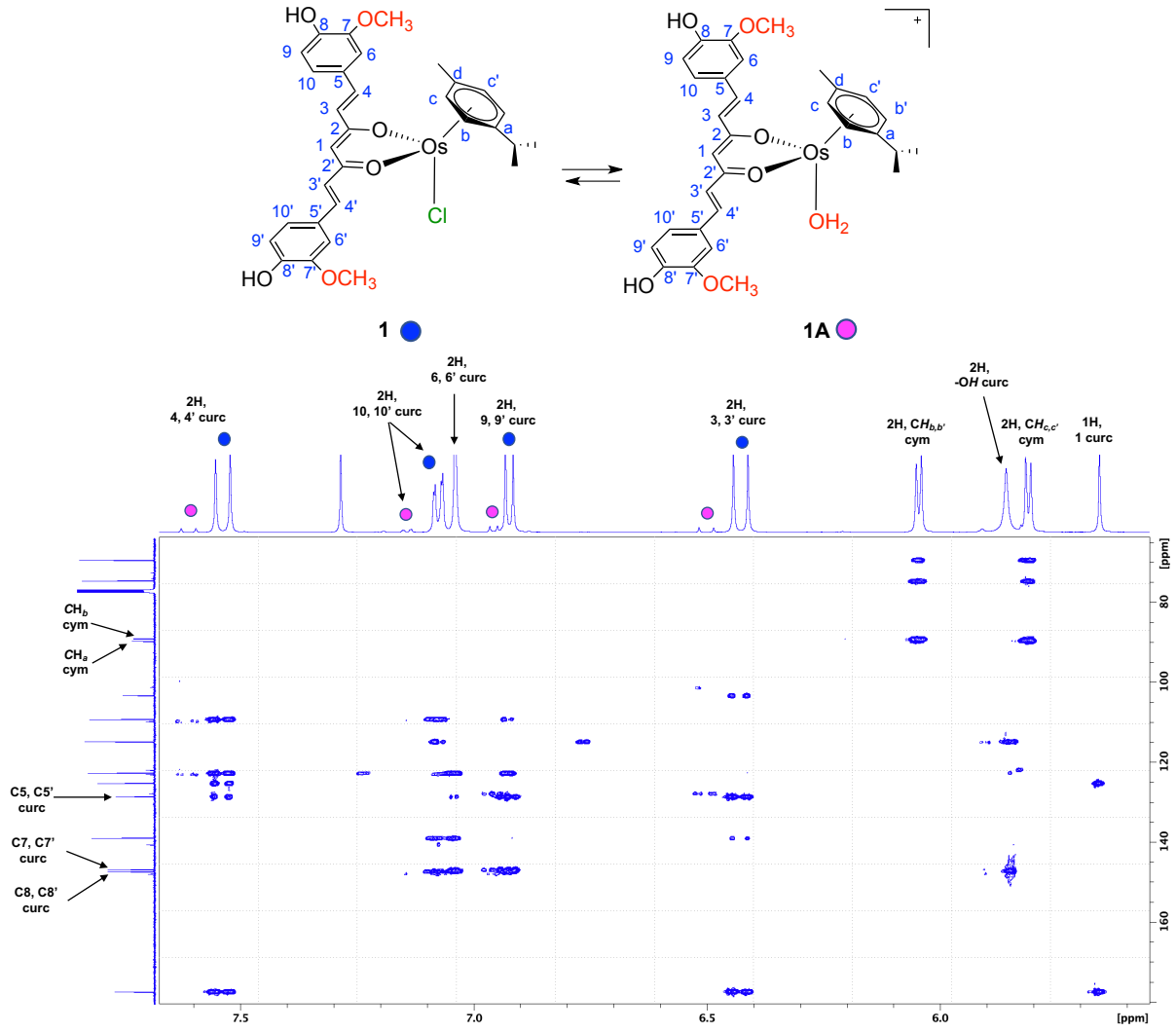

Figure S20. Magnification of {^{1}H, ^{13}C}-HMBC spectrum in $CDCl_3$ at 298 K of **1**.

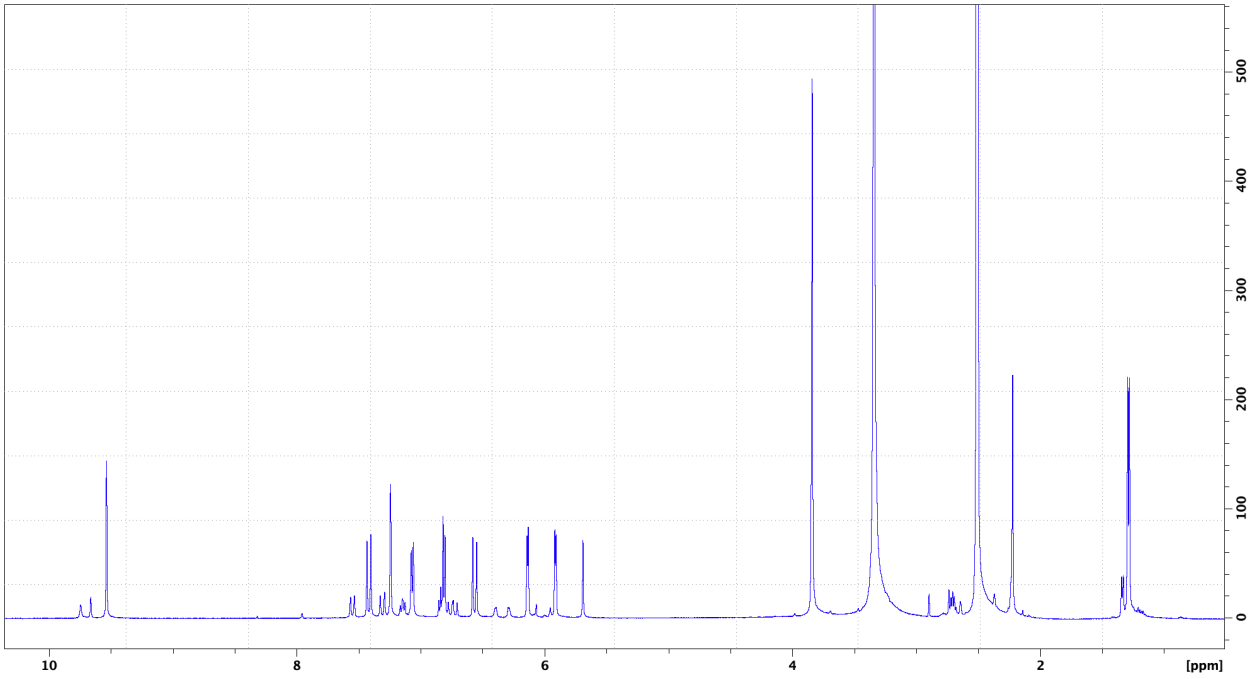

Figure S21. ^{1}H NMR spectrum in [D_6]DMSO at 298 K of **1**.

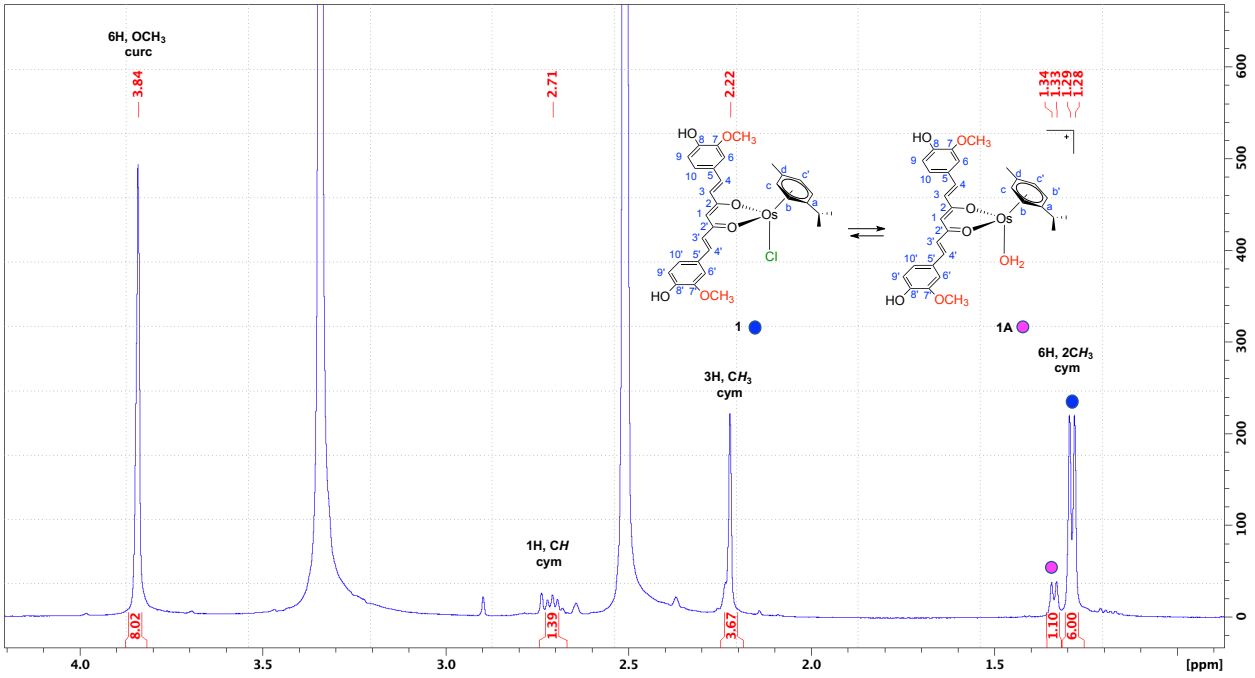

Figure S22. Magnification of ^{1}H NMR spectrum in [D_6]DMSO at 298 K of **1**.

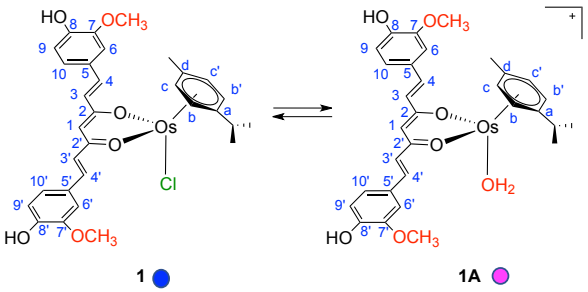

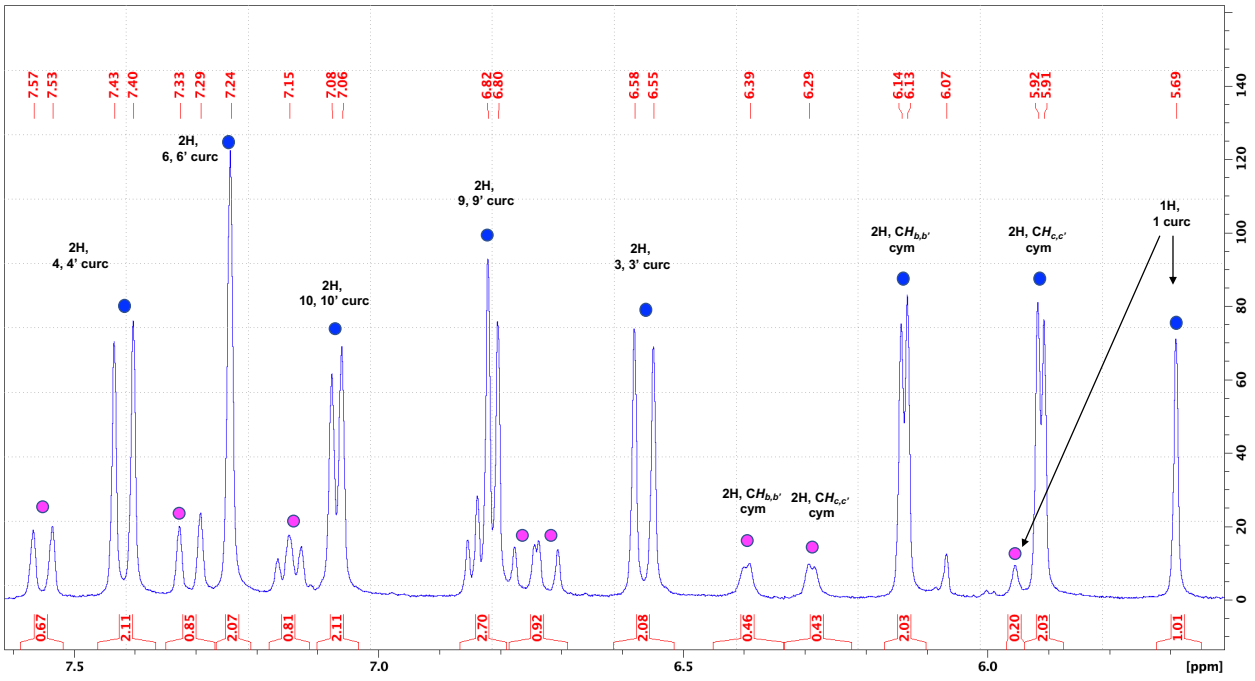

Figure S23. Magnification of ^{1}H NMR spectrum in [D_6]DMSO at 298 K of **1**.

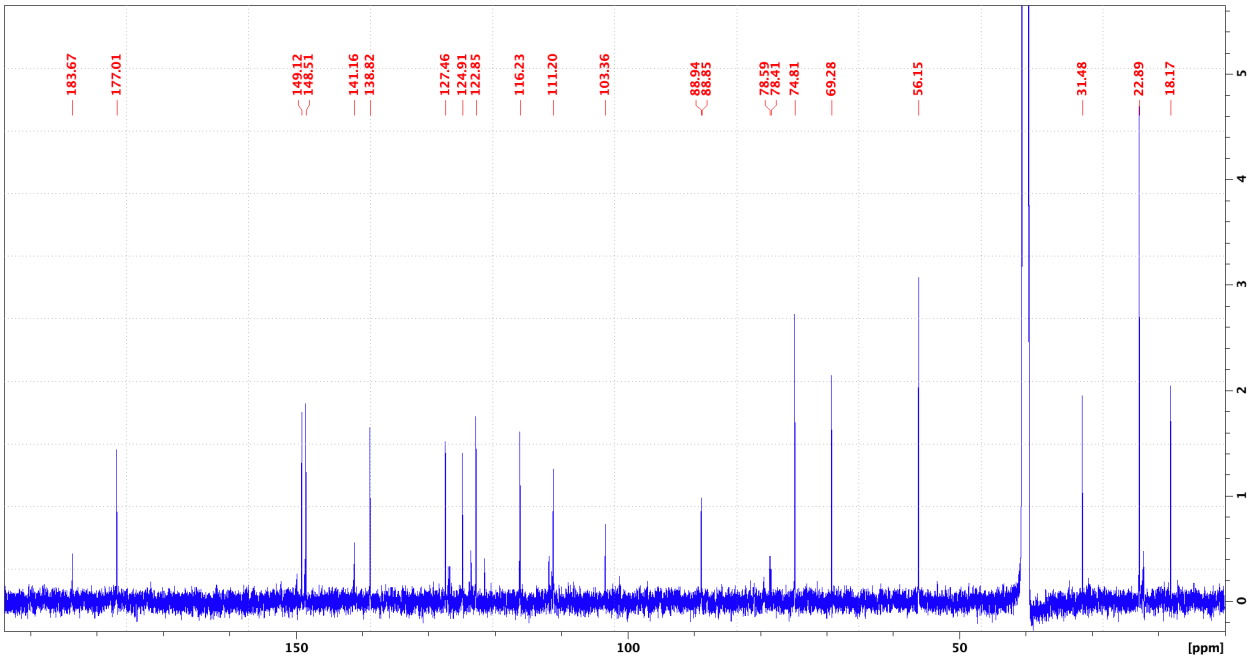

Figure S24. ^{13}C NMR spectrum in [D_6]DMSO at 298 K of **1**.

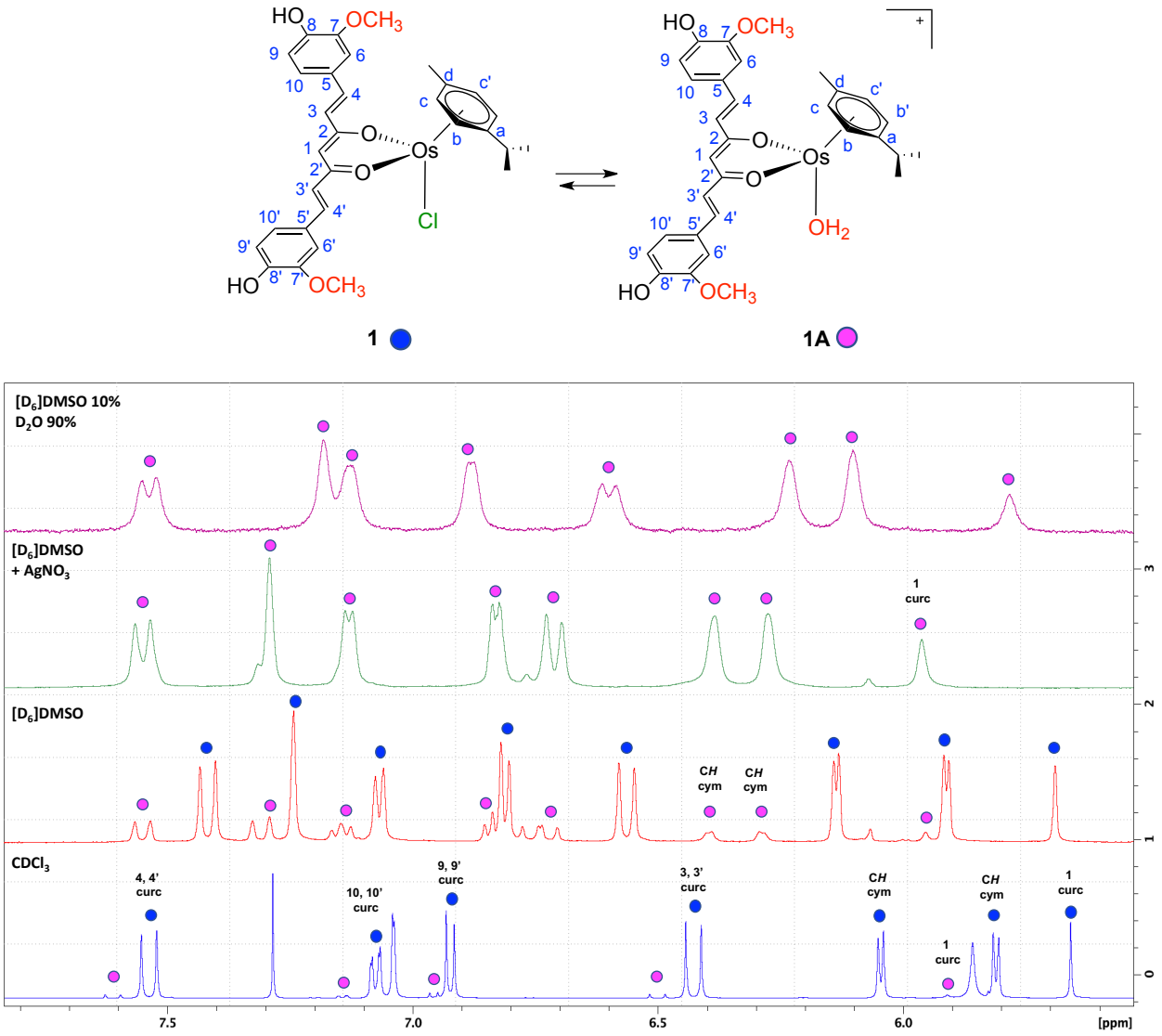

Figure S25. Low field region of the ^{1}H NMR spectra of **1**, [(p-cym)Os(curc)(Cl)]: (A) a solution of **1** in CD_3Cl at 298 K, (B) a solution of **1**, in DMSO [d_6] at 298 K and (C) after treatment of (B) with 1 mol equiv $AgNO_3$ for 1 h to remove the Cl ligand and generate **1A**, $[(p\text{-cym})Os(curc)(OH_2)]^+$ and (D) a solution of **1**, in 10% [D_6]DMSO-90% D_2O at 298 K.

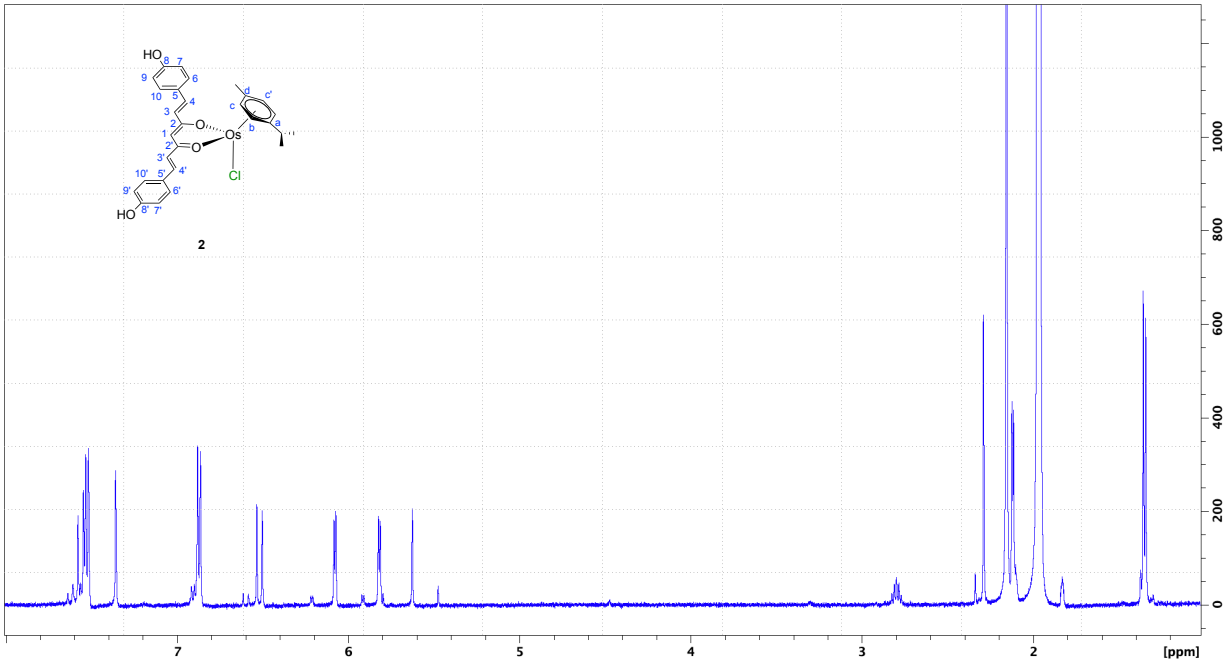

Figure S26. ^{1}H NMR spectrum in CD_3CN at 298 K of **2**.

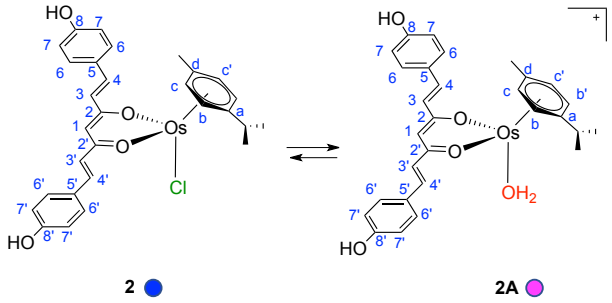

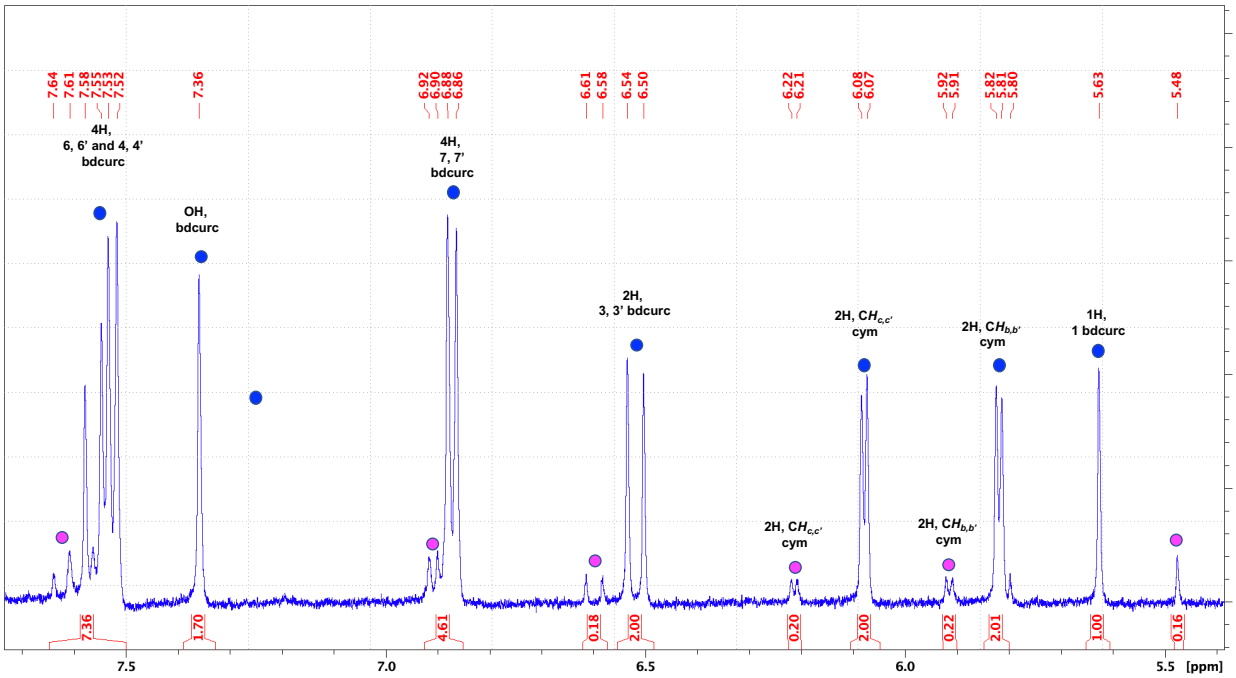

Figure S27. Magnification of ^{1}H NMR spectrum in CD_3CN at 298 K of **2**.

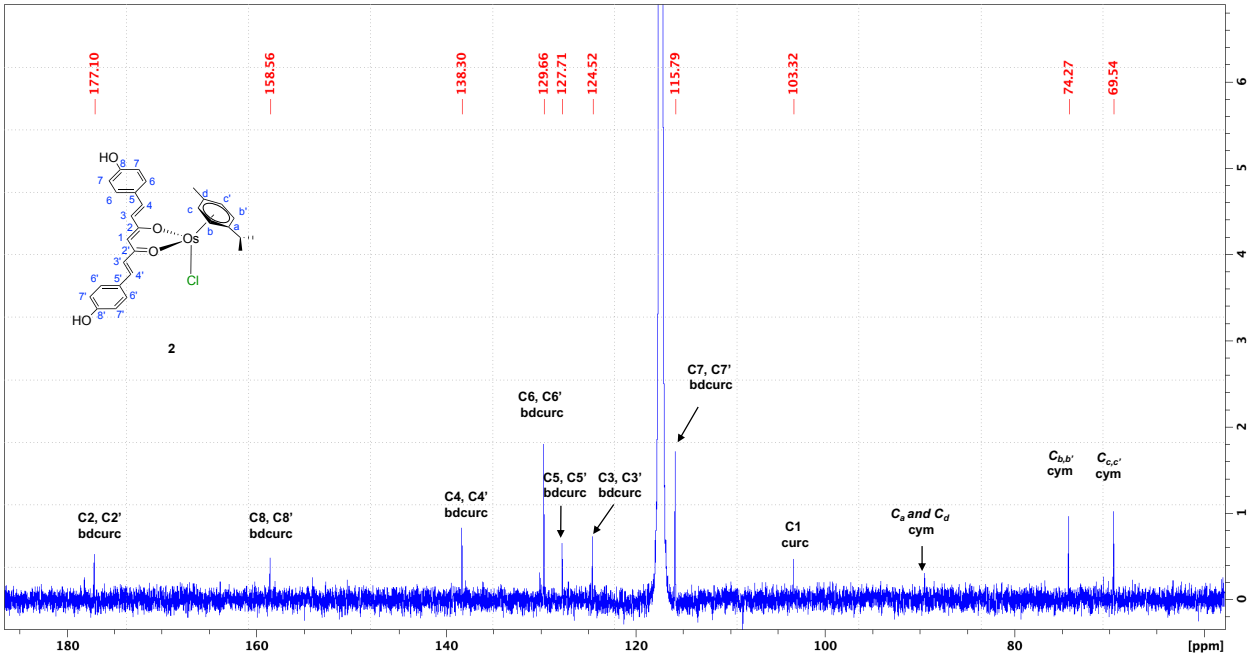

Figure S28. Magnification of ^{13}C NMR spectrum in CD_3CN at 298 K of **2**.

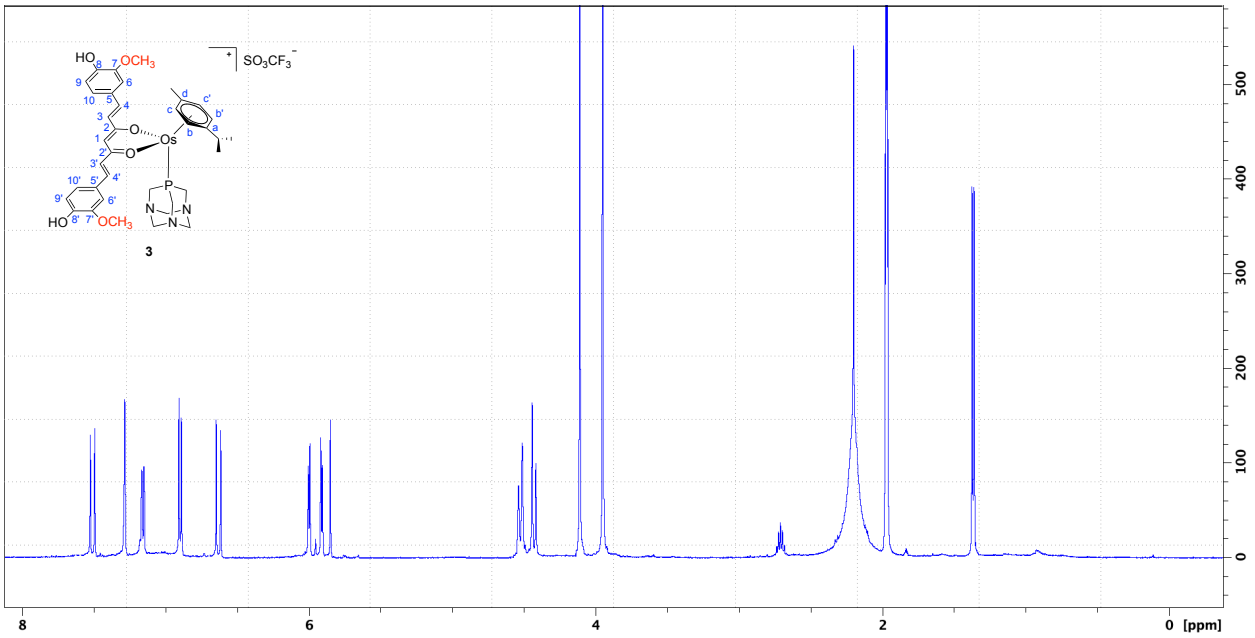

Figure S29. ^{1}H NMR spectrum in CD_3CN at 298 K of **3**.

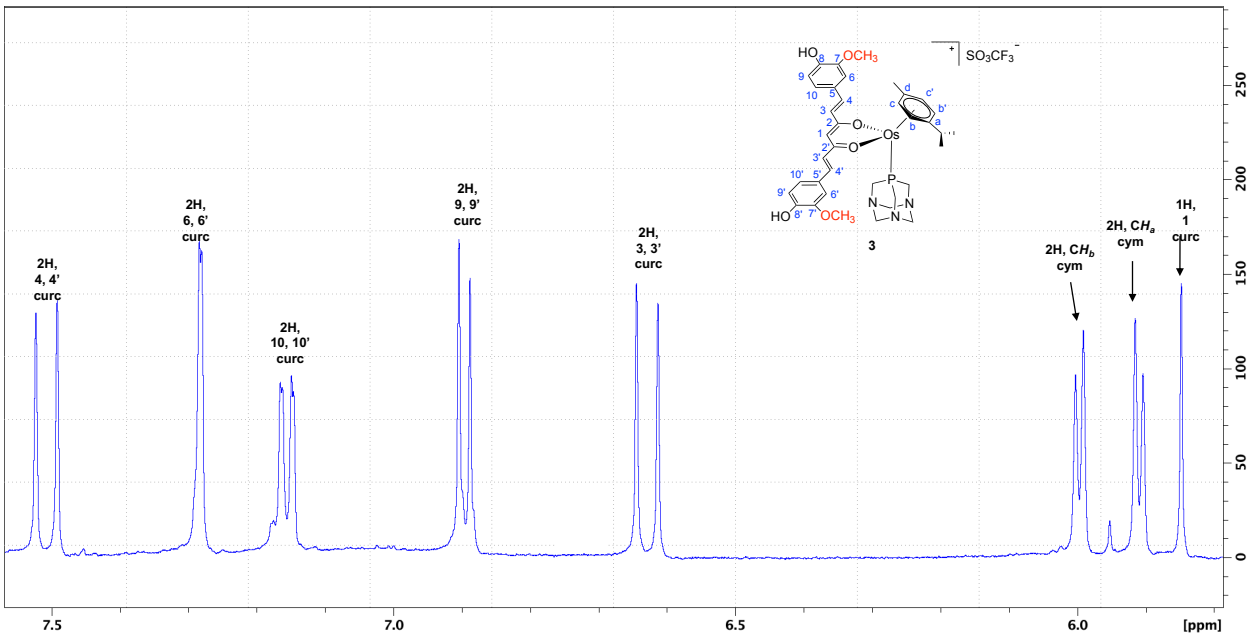

Figure S30. Magnification of ^{1}H NMR spectrum in CD_3CN at 298 K of **3**.

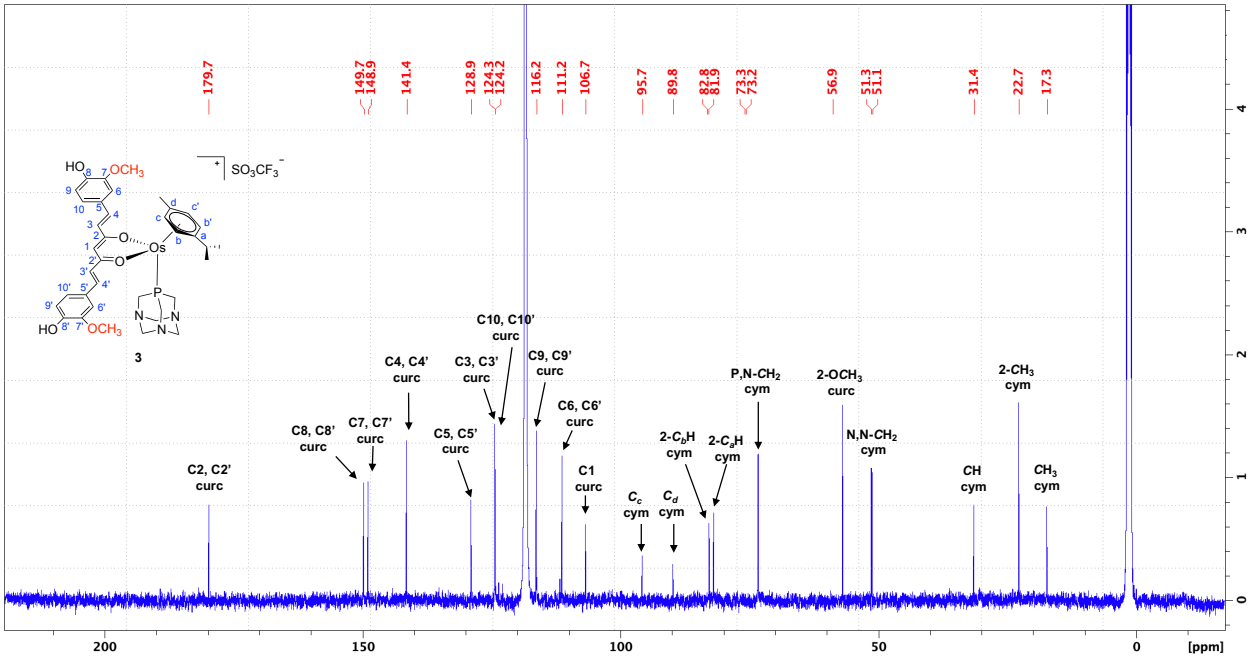

Figure S31. ^{13}C NMR spectrum in CD_3CN at 298 K of **3**.

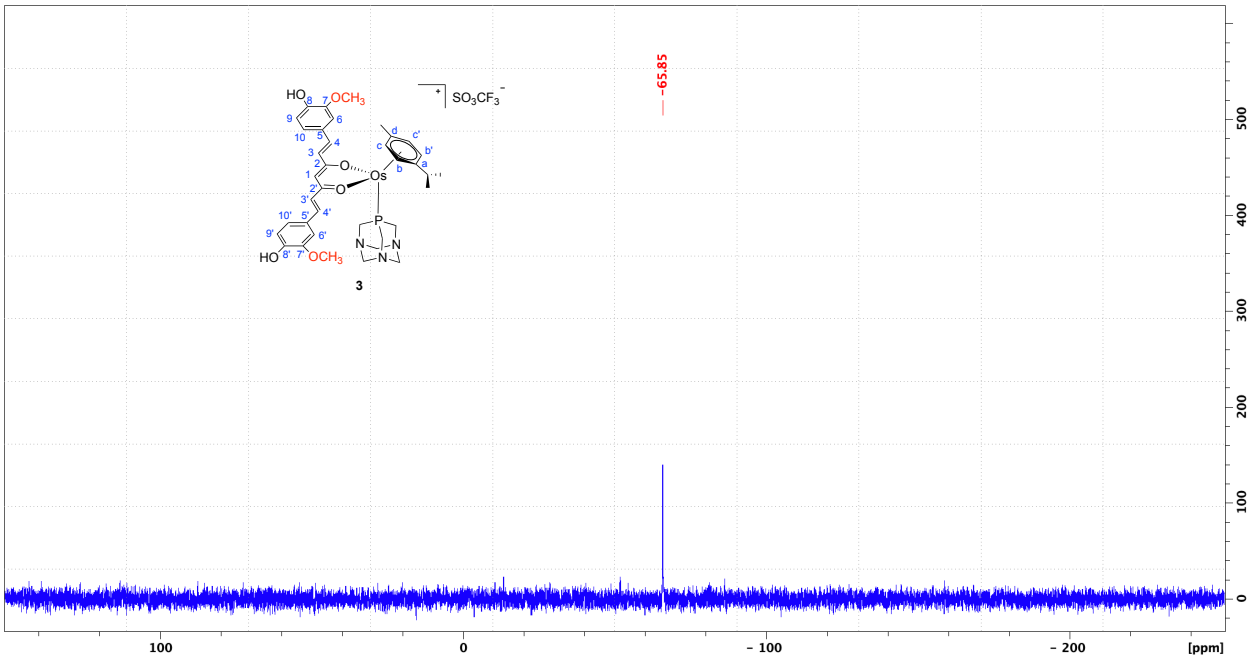

Figure S32. ^{31}P NMR spectrum in CD_3CN at 298 K of **3**.

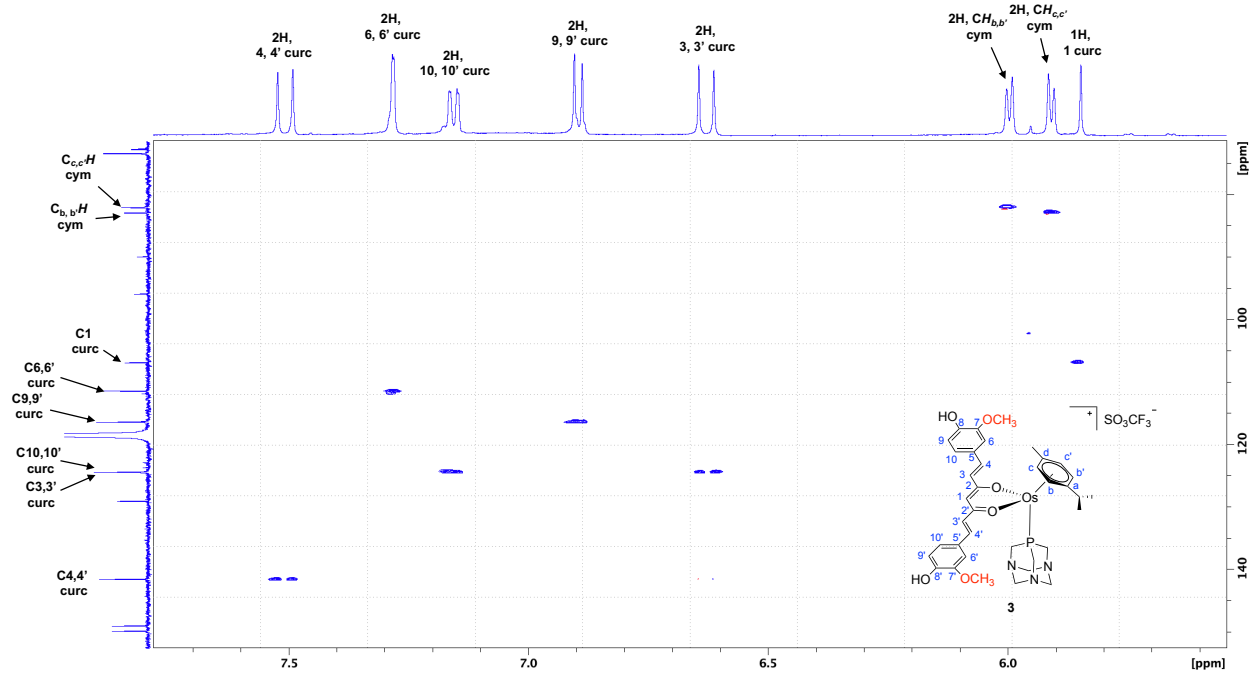

Figure S33. Magnification of {^{1}H, ^{13}C}-HSQC spectrum in CD_3CN at 298 K of **3**.

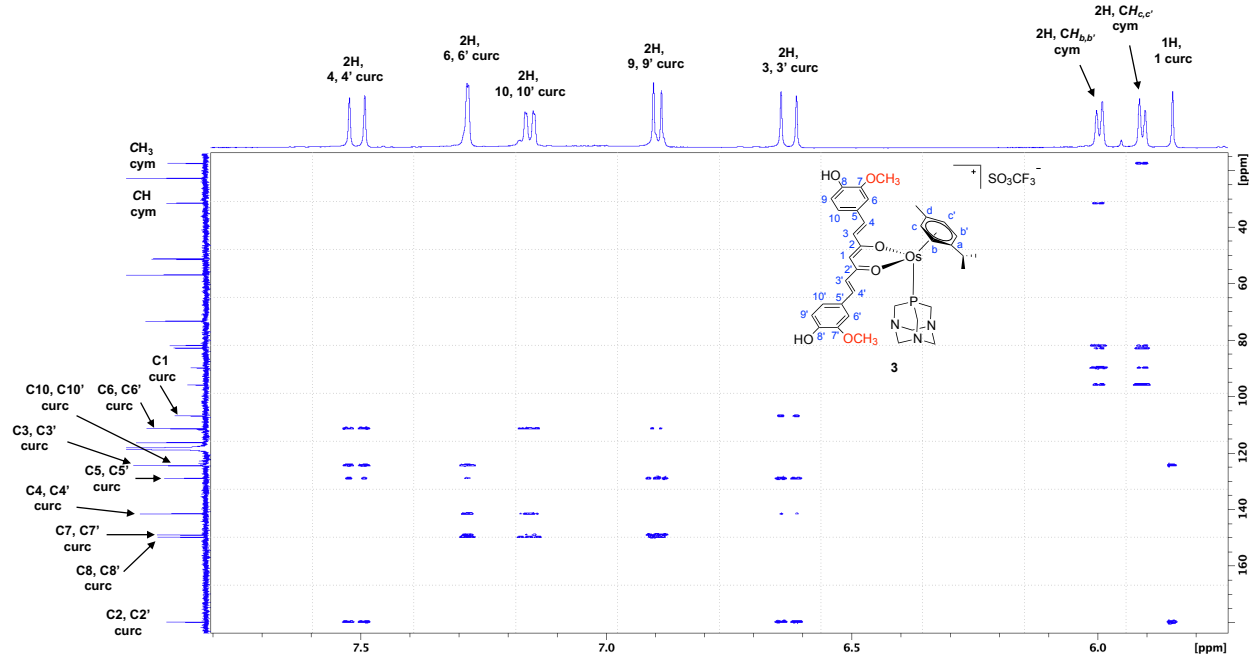

Figure S34. Magnification of {^{1}H, ^{13}C}-HMBC spectrum in CD_3CN at 298 K of **3**.

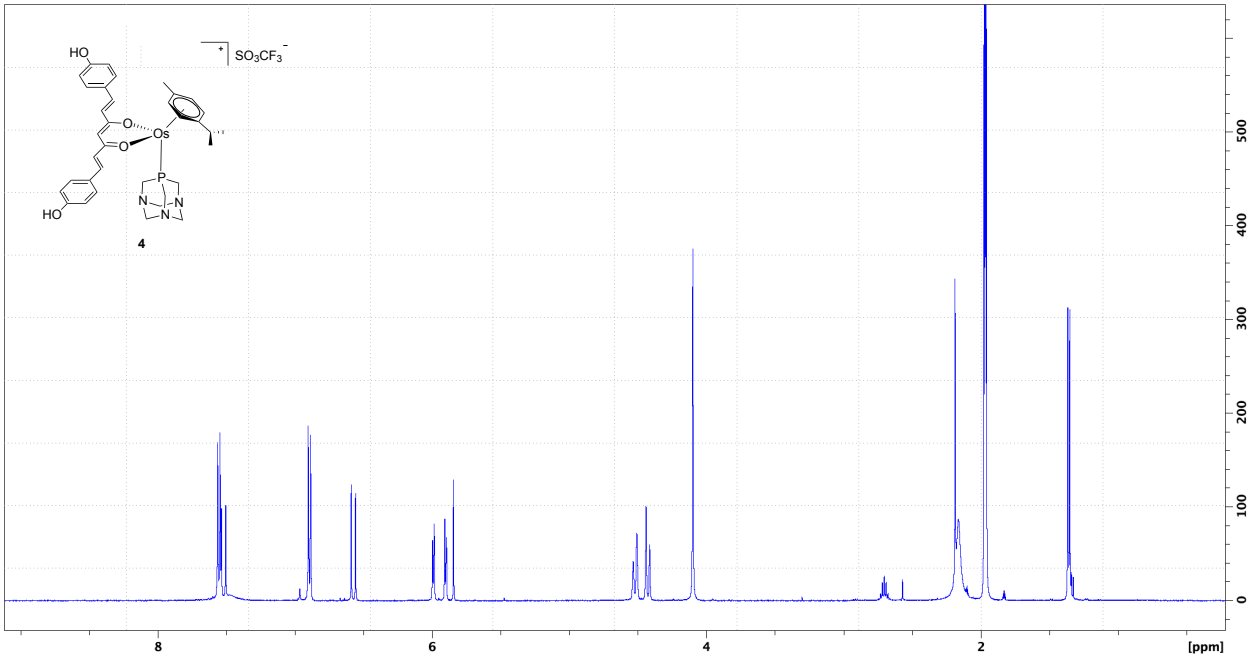

Figure S35. ^{1}H NMR spectrum in CD_3CN at 298 K of **4**.

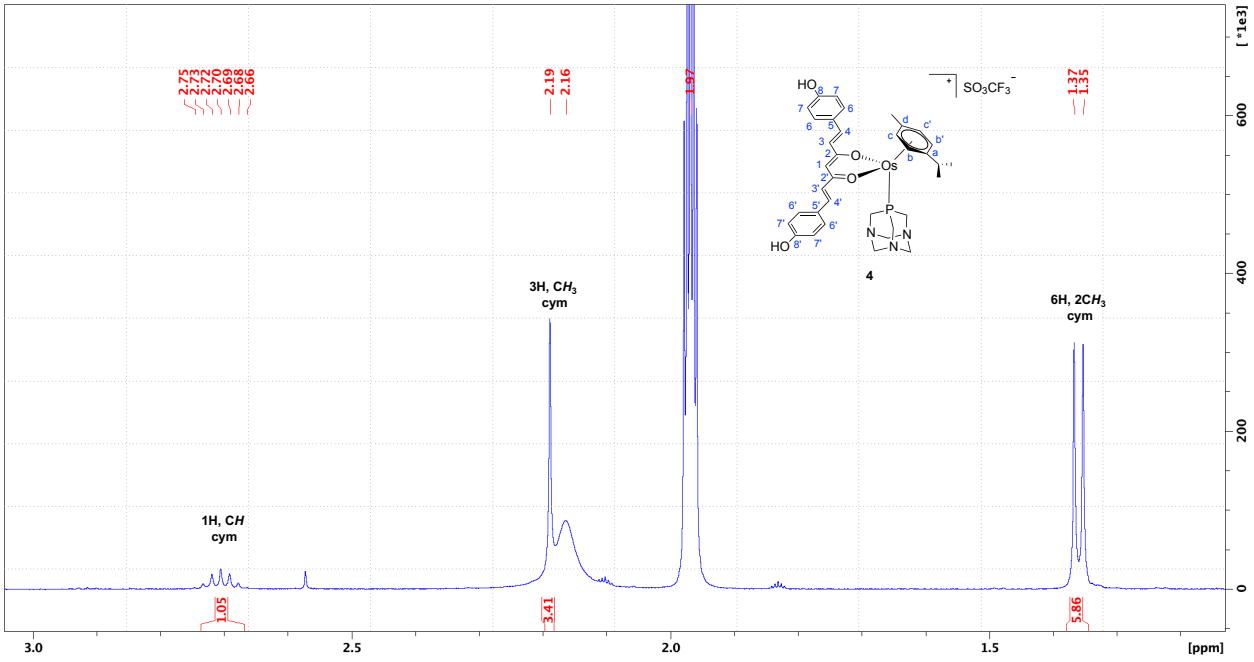

Figure S36. Magnification of ^{1}H NMR spectrum in CD_3CN at 298 K of **4**.

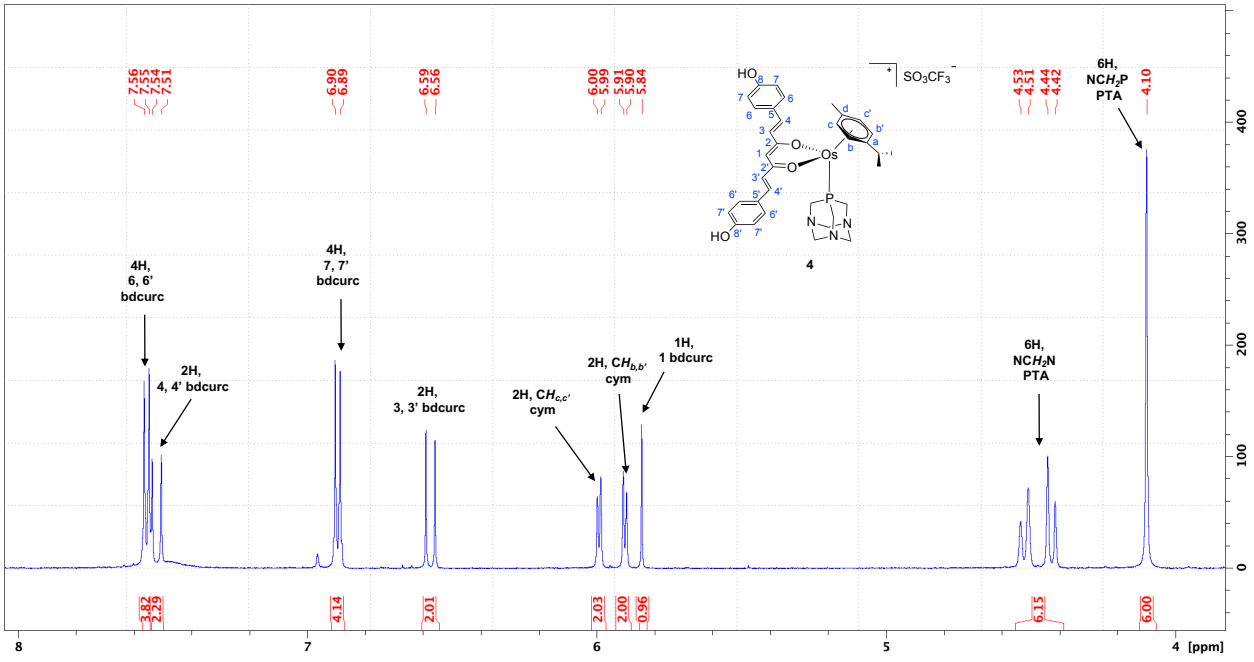

Figure S37. Magnification of ^{1}H NMR spectrum in CD_3CN at 298 K of **4**.

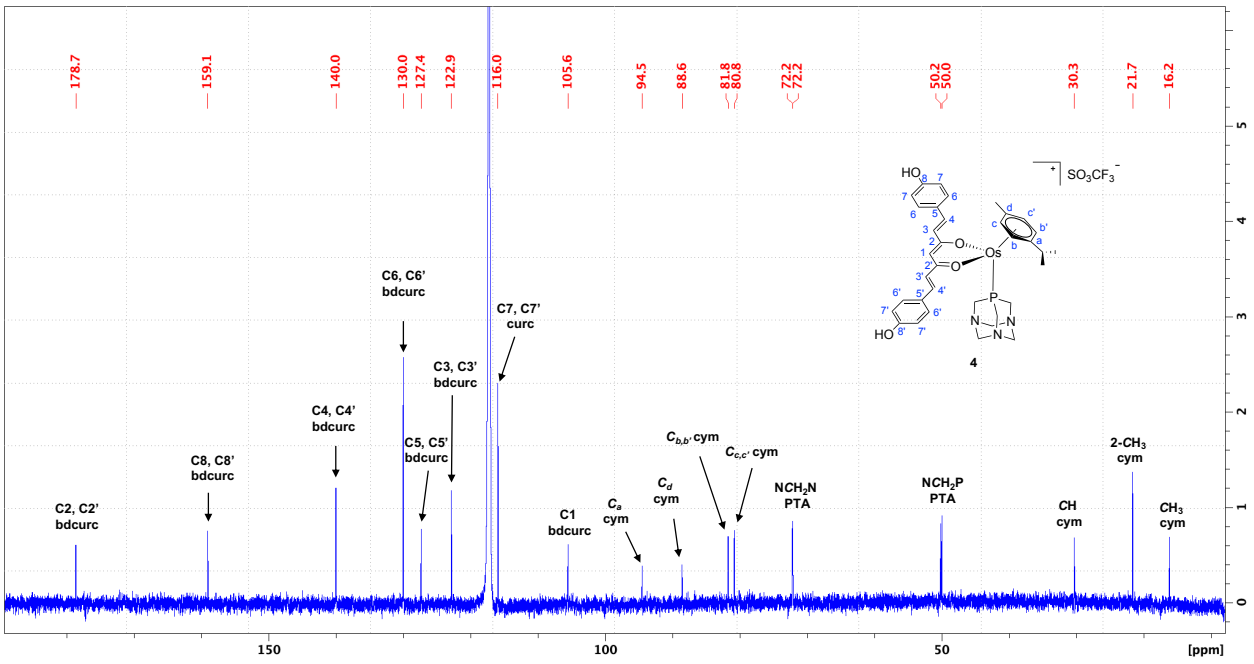

Figure S38. ^{13}C NMR spectrum in CD_3CN at 298 K of **4**.

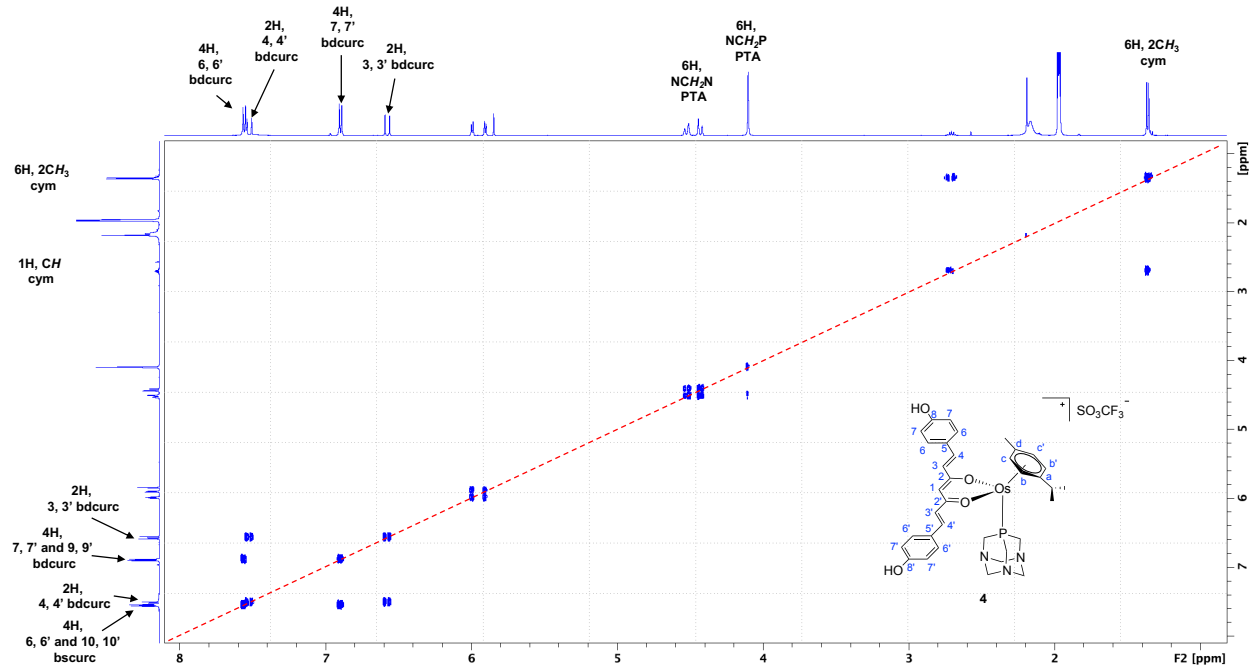

Figure S39. {^{1}H, ^{1}H}-COSY spectrum in $CDCl_3$ at 298 K of **4**.

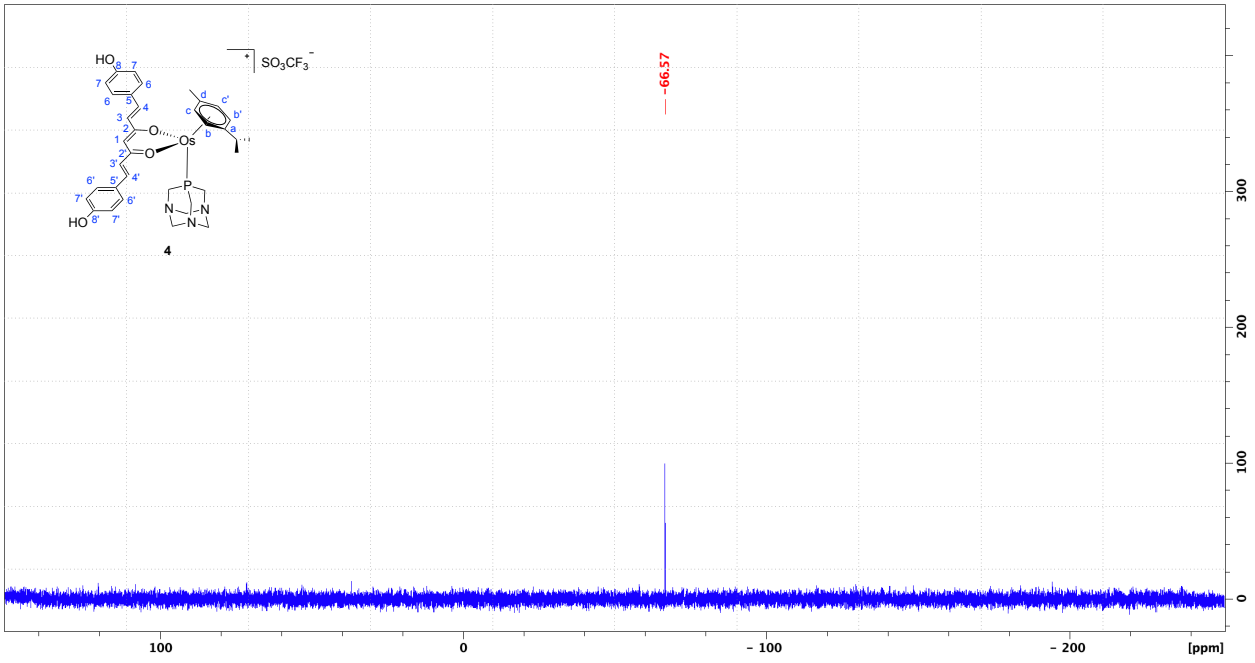

Figure S40. ^{31}P NMR spectrum in CD_3CN at 298 K of **4**.

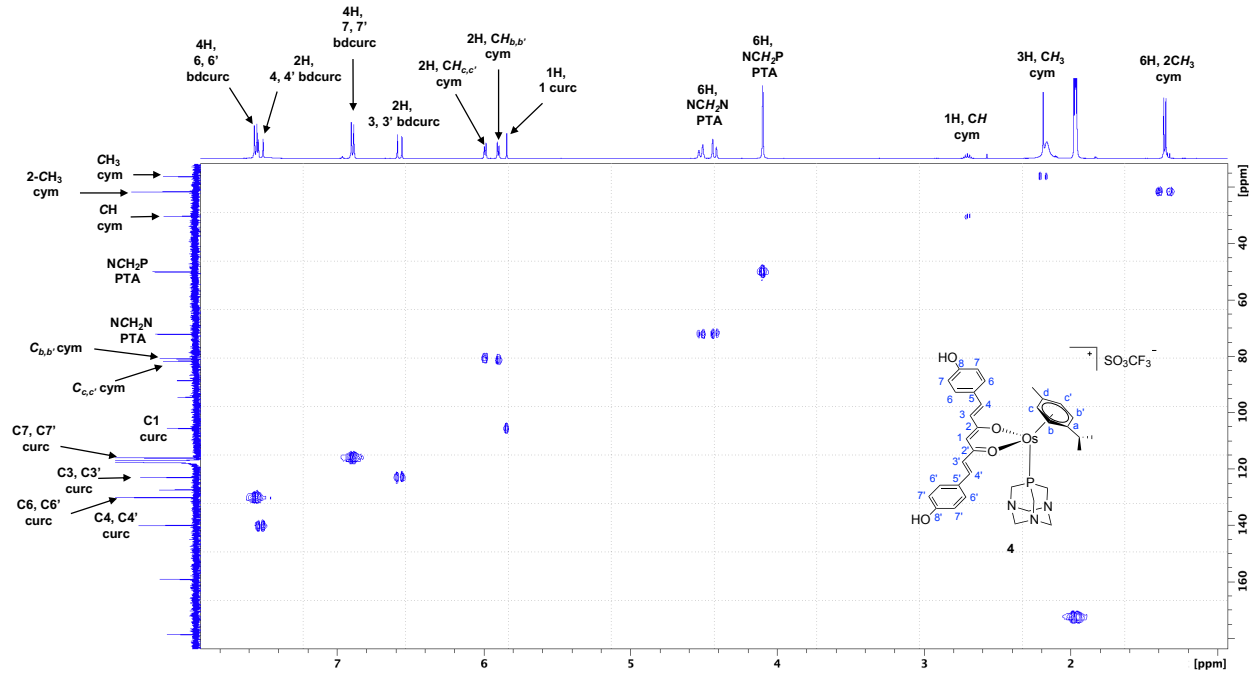

Figure S41. {^{1}H, ^{13}C}-HSQC spectrum in CD_3CN at 298 K of **4**.

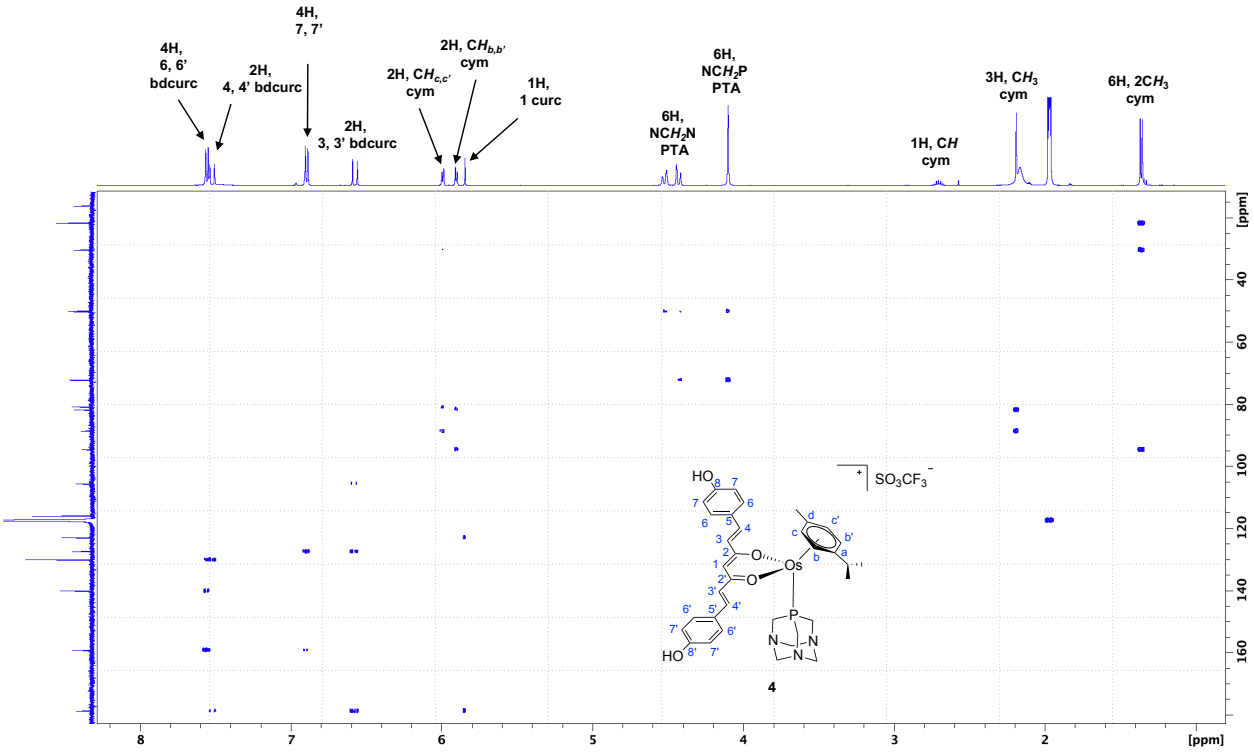

Figure S42. {^{1}H, ^{13}C}-HMBC spectrum in CD_3CN at 298 K of **4**.

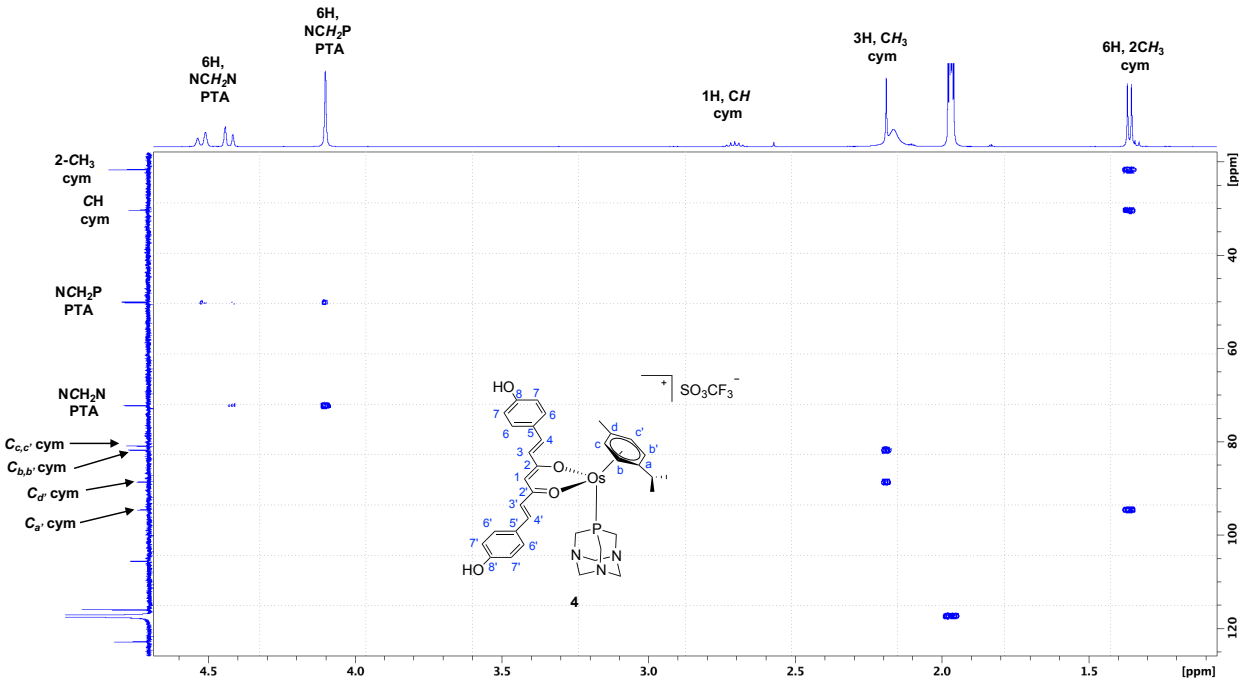

Figure S43. Magnification of {^{1}H, ^{13}C}-HMBC spectrum in CD_3CN at 298 K of **4**.

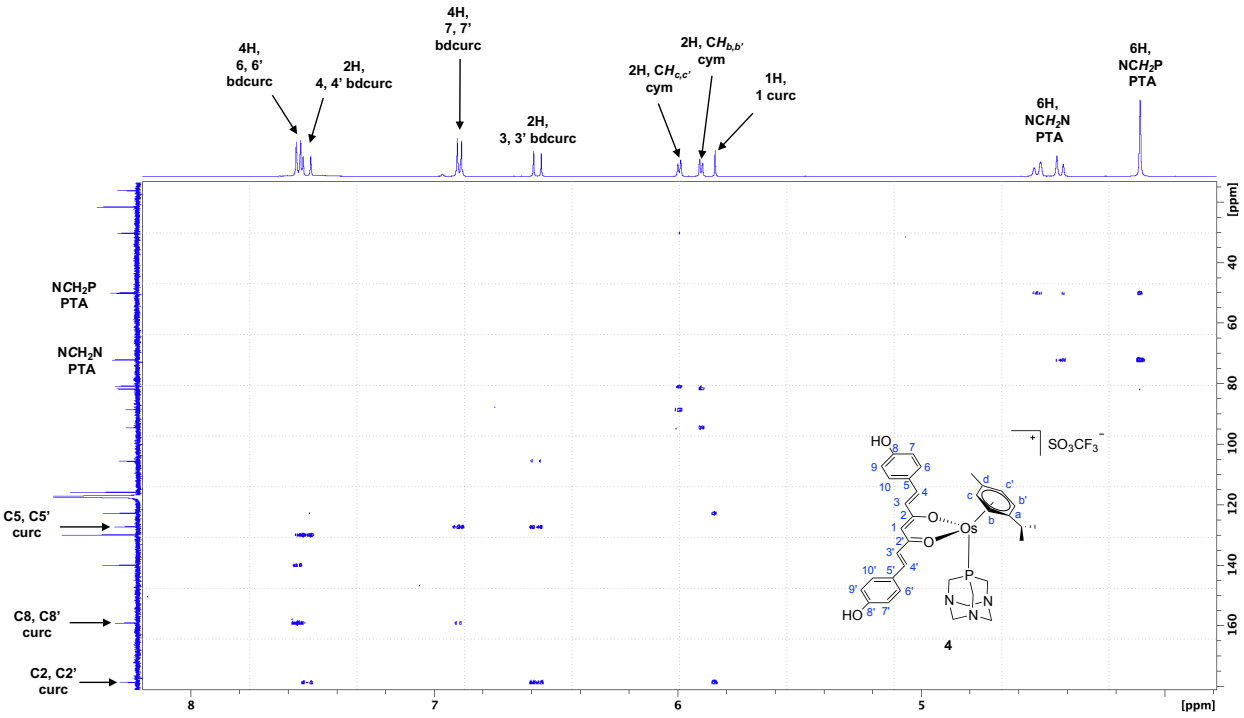

Figure S44. Magnification of {^{1}H, ^{13}C}-HMBC spectrum in CD_3CN at 298 K of **4**.

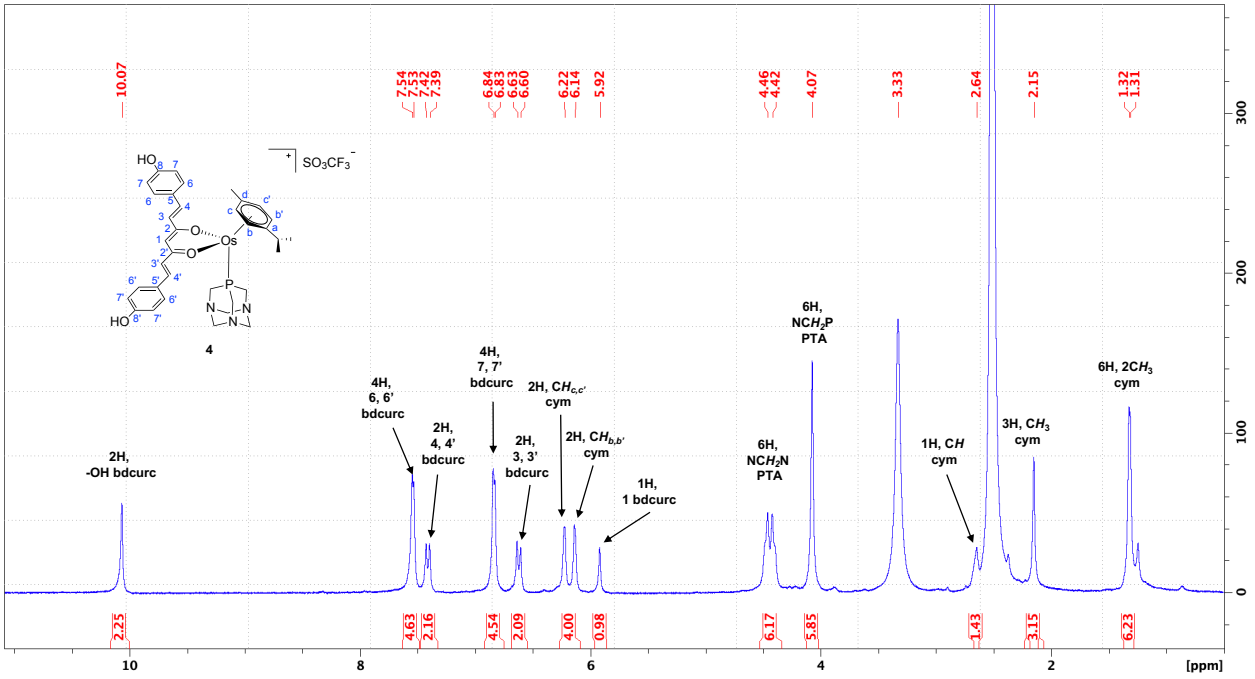

Figure S45. ^{1}H NMR spectrum in [D_6]DMSO at 298 K of **4**.

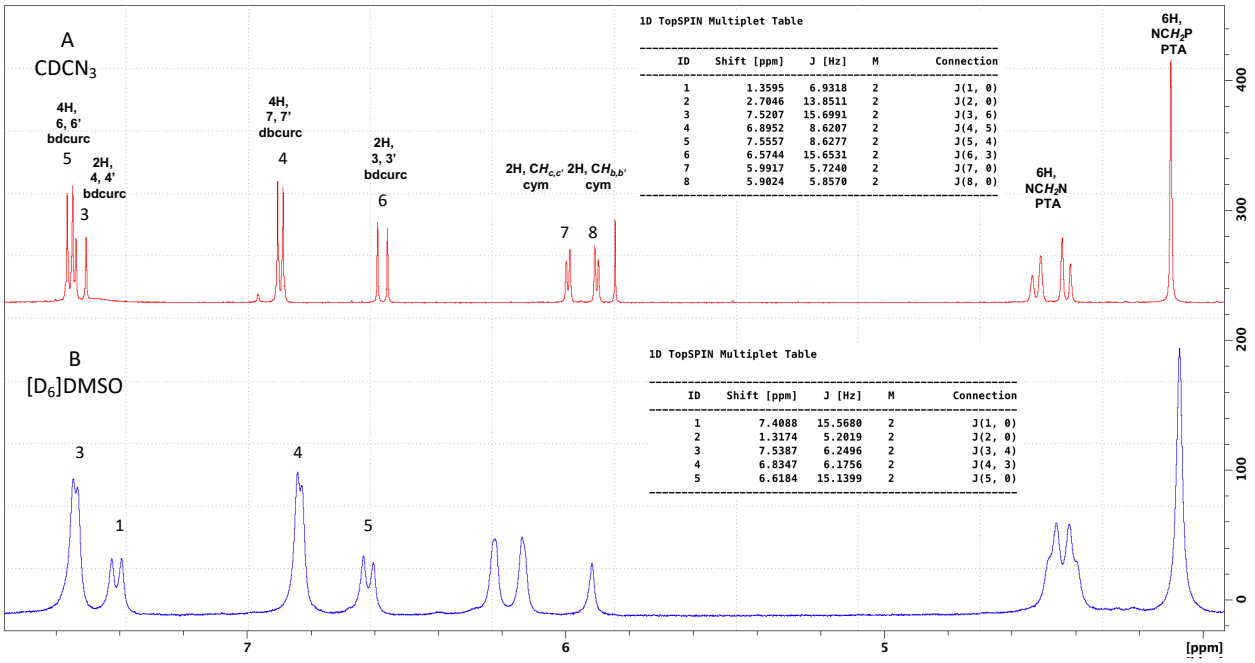

Figure S46. Low field region of the ^{1}H NMR spectra of **4**, [(p-cym)Os(bdcurc)PTA]: (A) a solution of **4** in CD_3CN at 298 K, (B) a solution of **4**, in [D_6] DMSO at 298 K and.

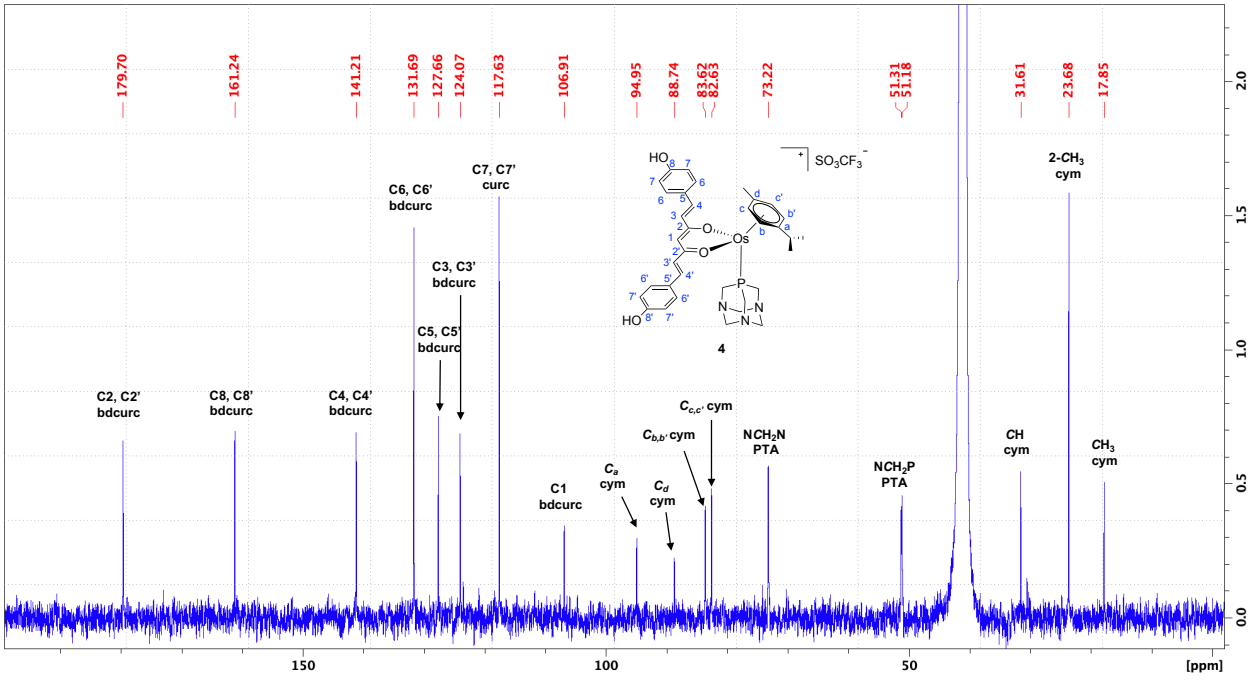

Figure S47. ^{13}C NMR spectrum in [D_6] DMSO at 298 K of **4**.

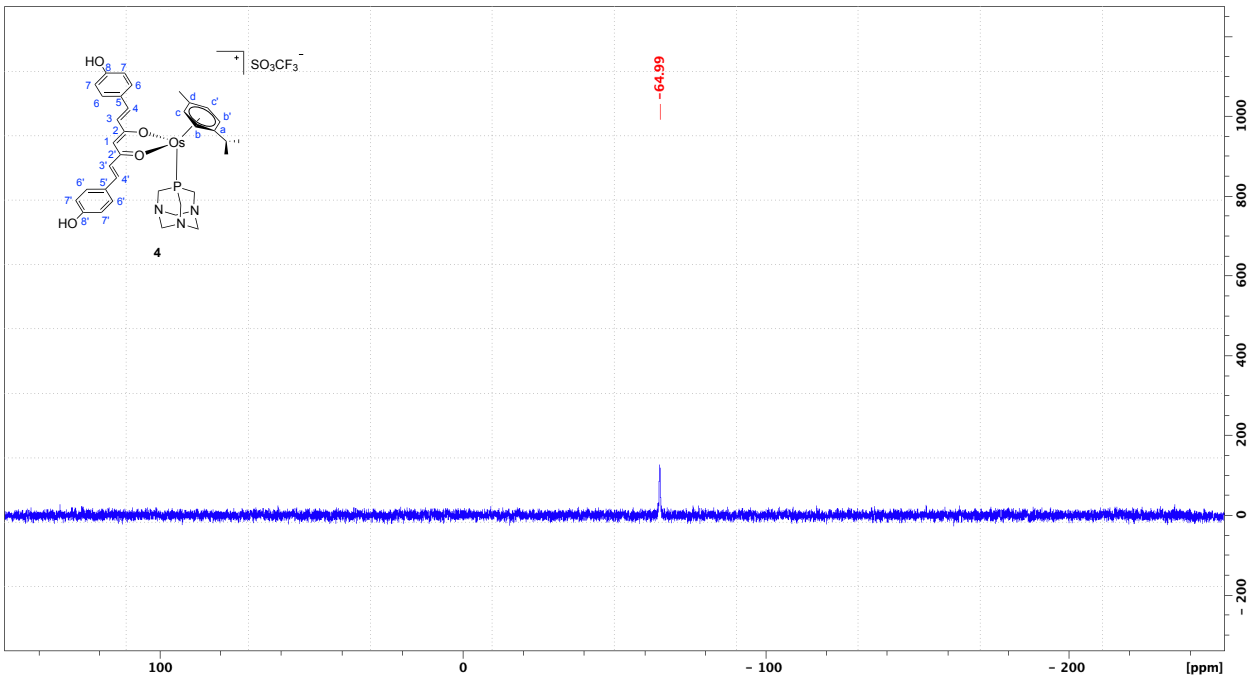

Figure S48. ^{31}P NMR spectrum in [D_6] DMSO at 298 K of **4**.

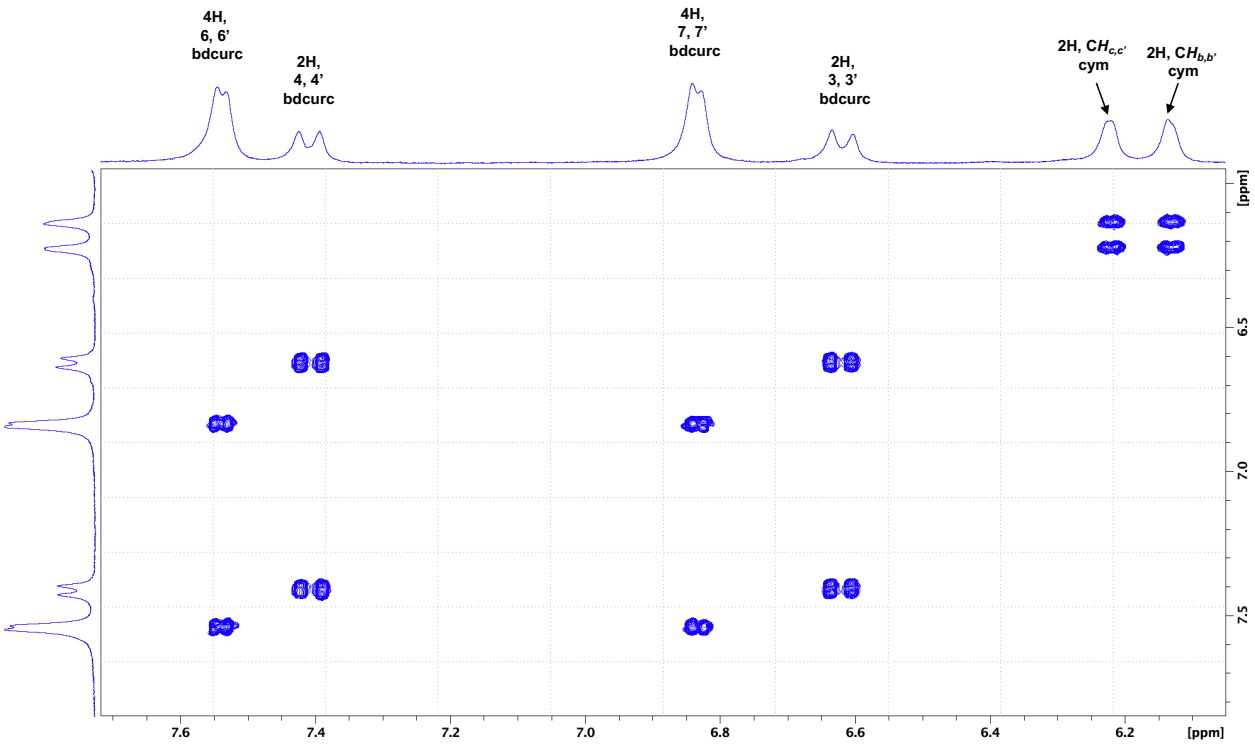

Figure S49. Magnification of {^{1}H, ^{1}H}-COSY spectrum [D_6] DMSO at 298 K of **4**.

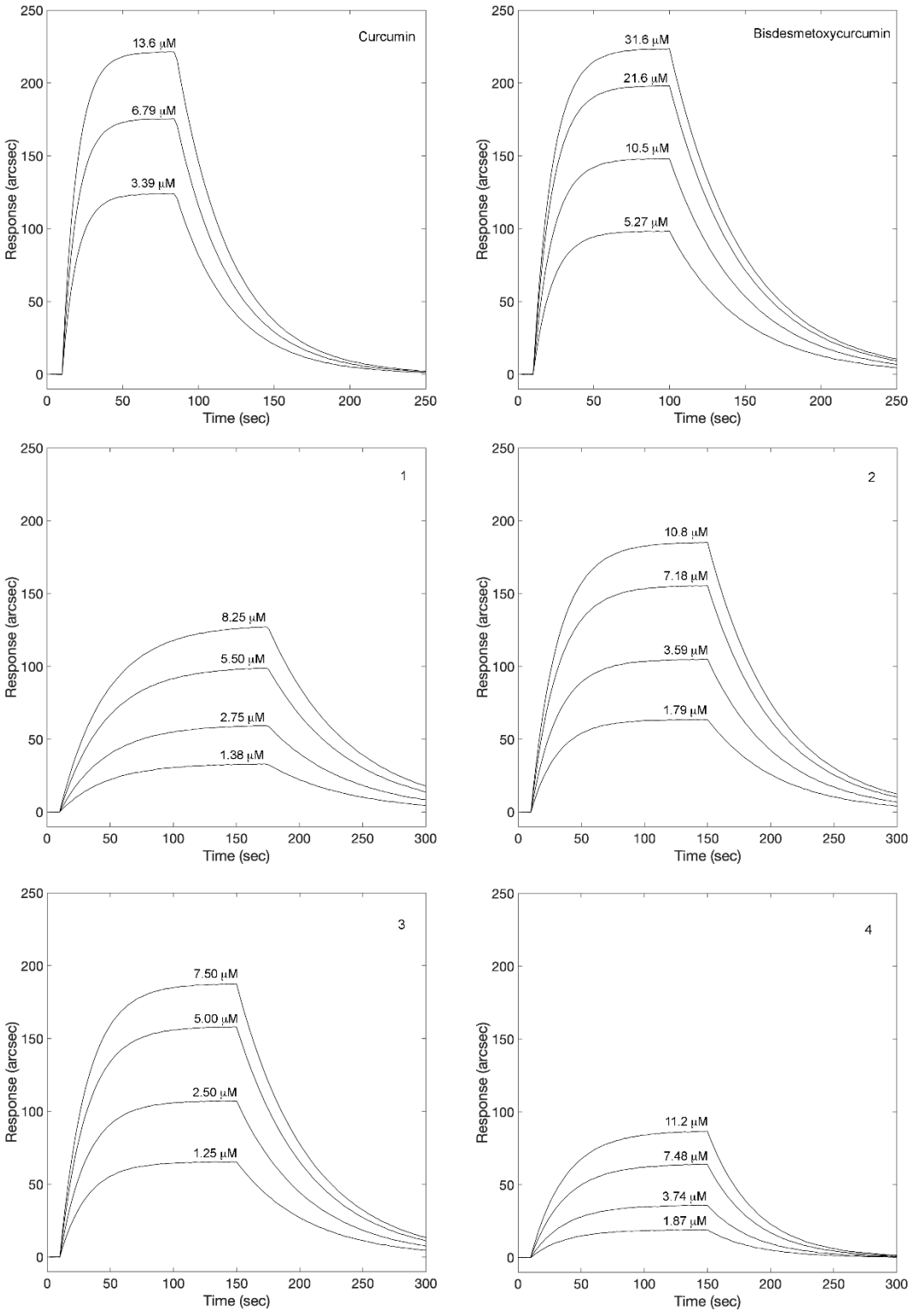

Fig. S50. Superimpositions of mono-exponential binding curves obtained upon independent additions of different concentrations of curcH, bdcurcH and compounds **1-4** to surface-blocked DNA.

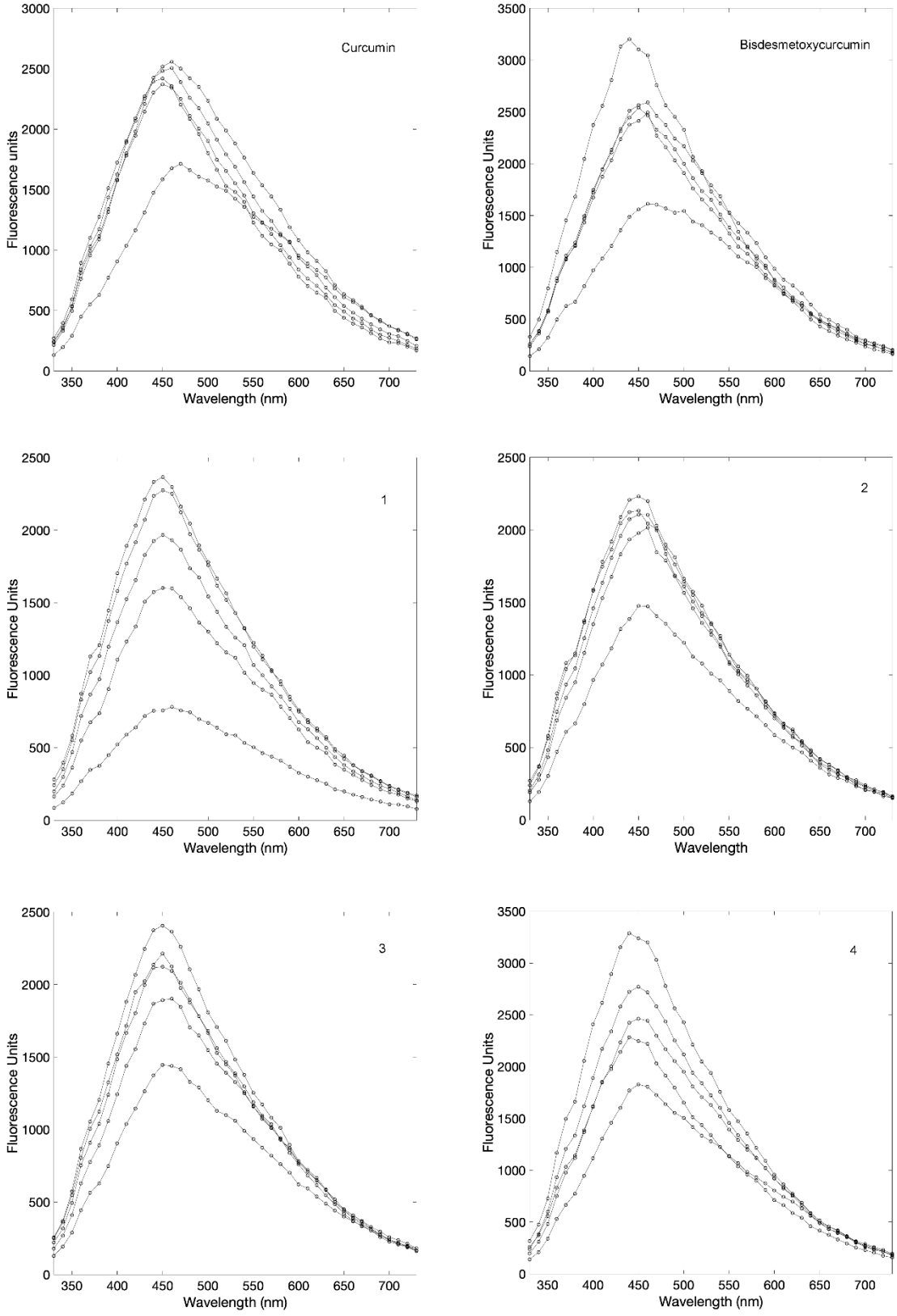

Fig. S51. Changes in fluorescence emission spectra of DAPI-DNA complex solution upon excitation at 338 nm (upper curves) in the presence of increasing concentration of curcH, bdcurcH and compounds **1**-**4** the range 0-100 μM.

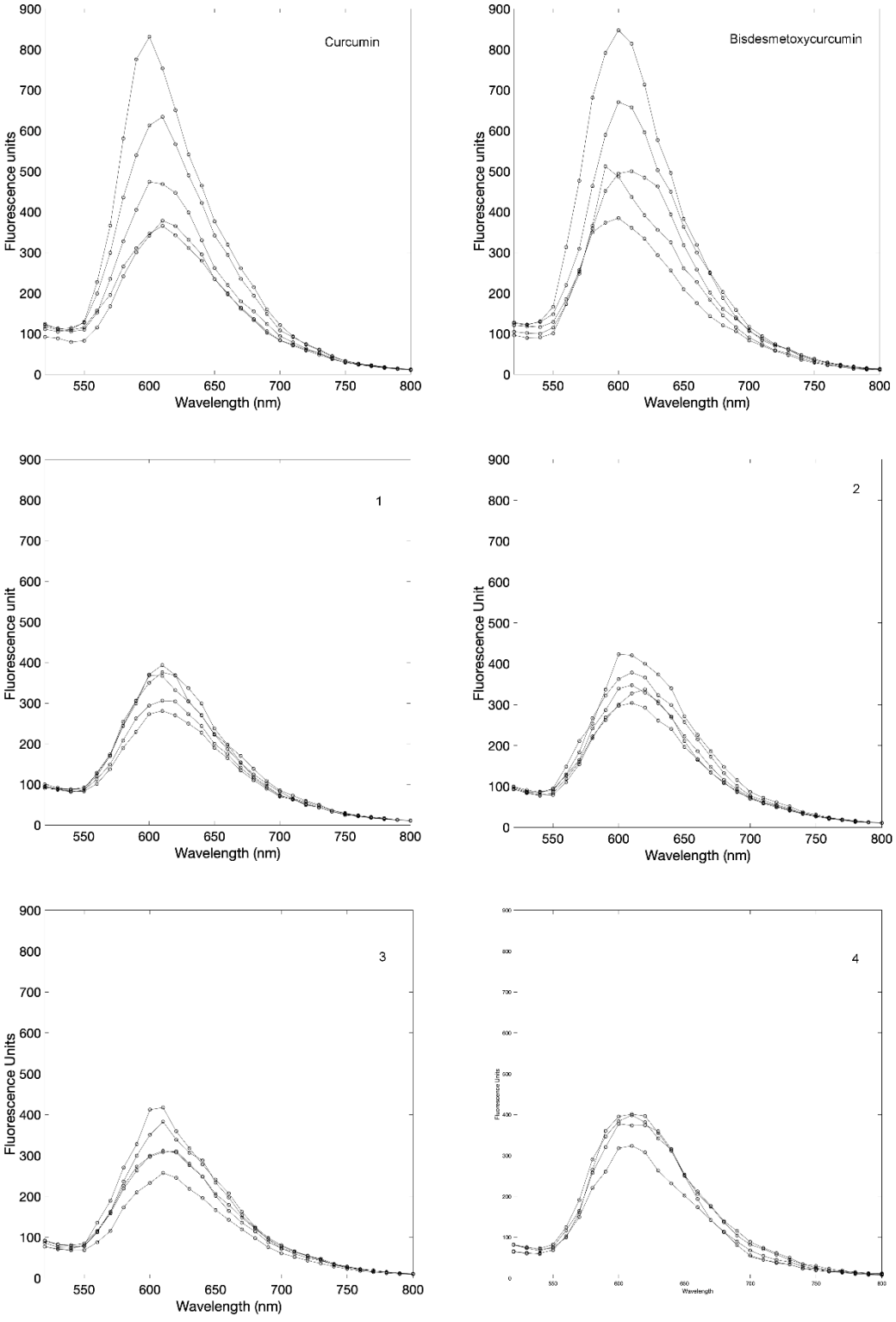

Fig. S52. Changes in fluorescence emission spectra of EtBr-DNA complex solution upon excitation at 500 nm (upper curves) in the presence of increasing concentration of curcH, bdcurcH and compounds **1**-**4** the range 0-100 μM. Only curcH and bdcurcH can displace EtBr molecule and intercalate DNA. No significant change is observed with compounds **1-4**.

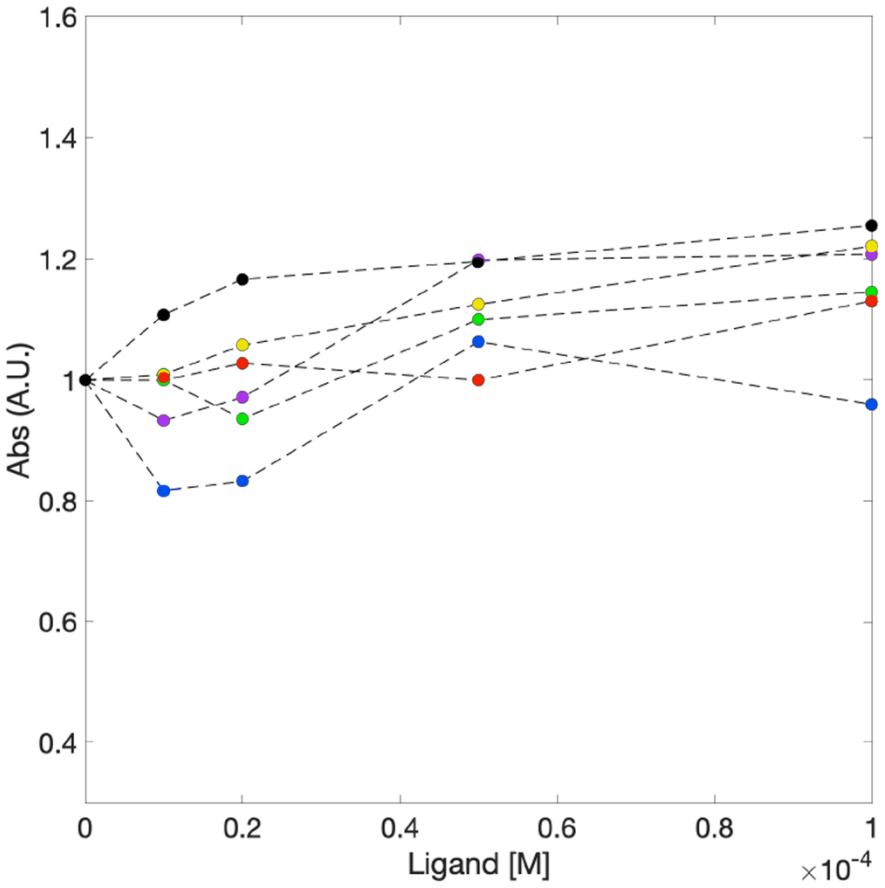

Fig. S53. Changes in absorbance at 630 nm of methyl green-DNA complex solution upon competition with increasing concentration of curcH (black), bdcurcH (blue) and compounds **1** (green), **2** (yellow), **3** (violet) and **4** (red) in the range 0-100 μM.

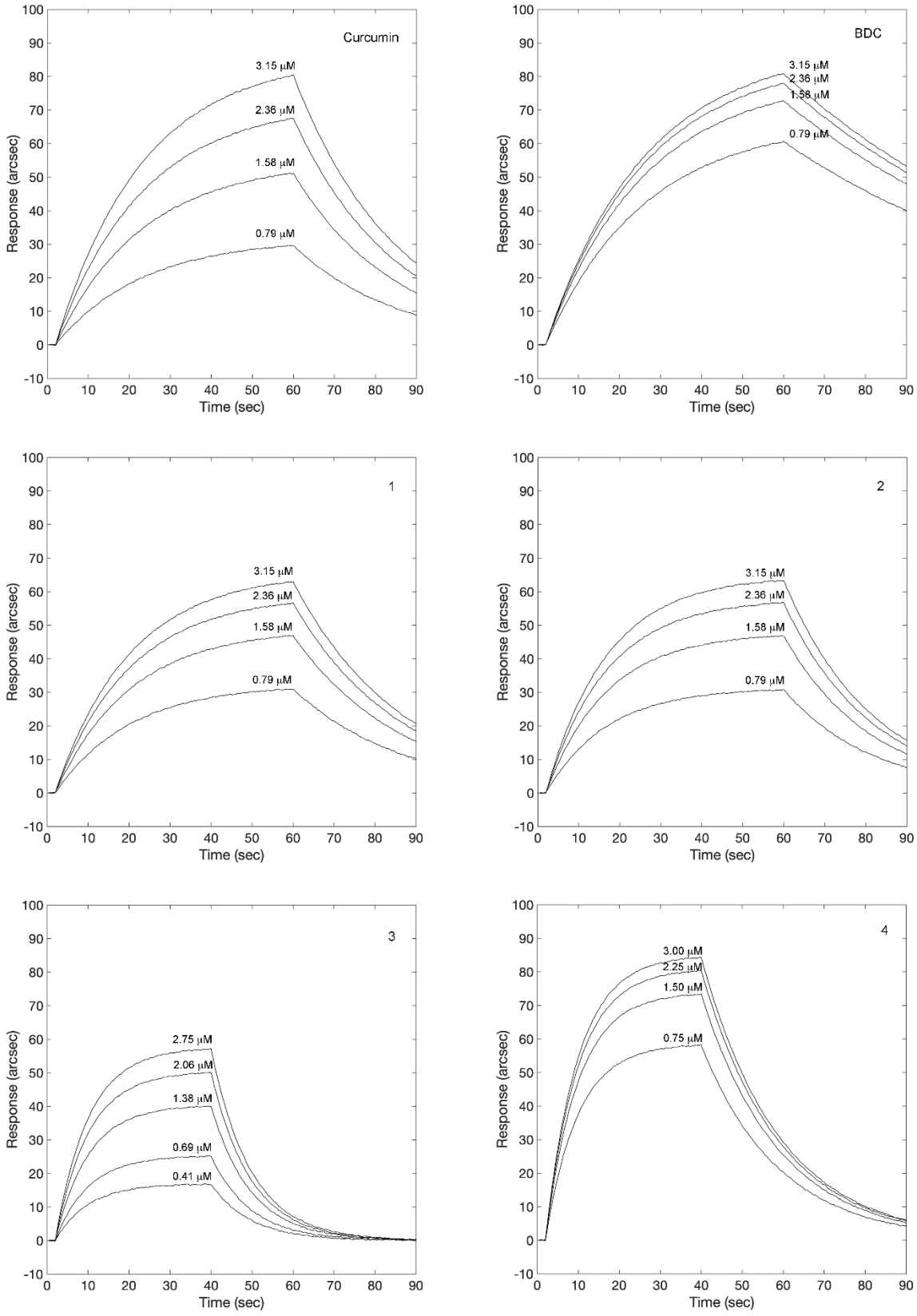

Fig. S54. Superimpositions of mono-exponential binding curves obtained upon independent additions of different concentrations of curcH, bdcurcH and compounds **1**-**4** to surface-blocked BSA.

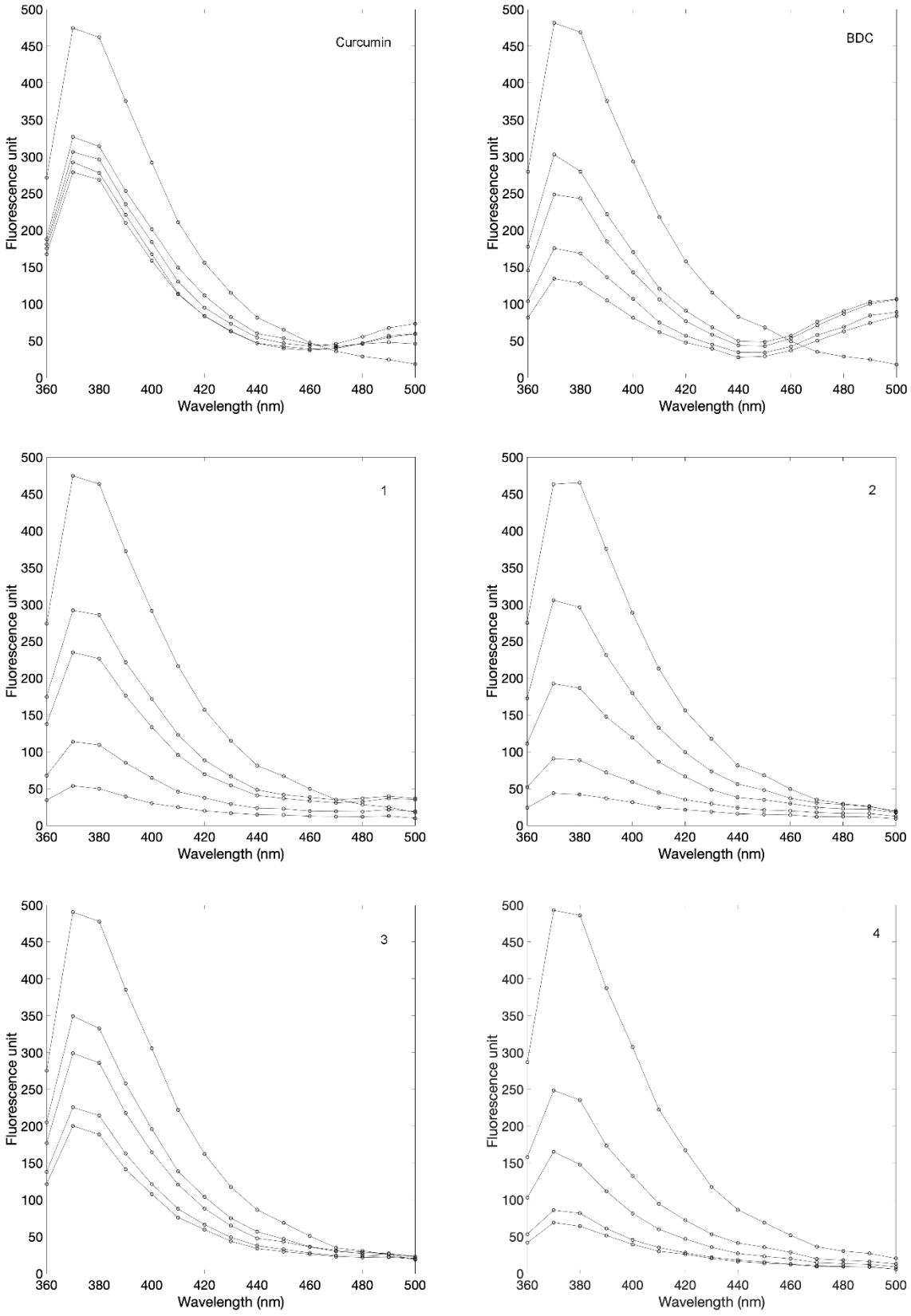

Fig. S55. Changes in fluorescence emission spectra of BSA (upper curves) upon titration with curcH, bdcurcH, and **1**-**4** the range 0-100 μM.

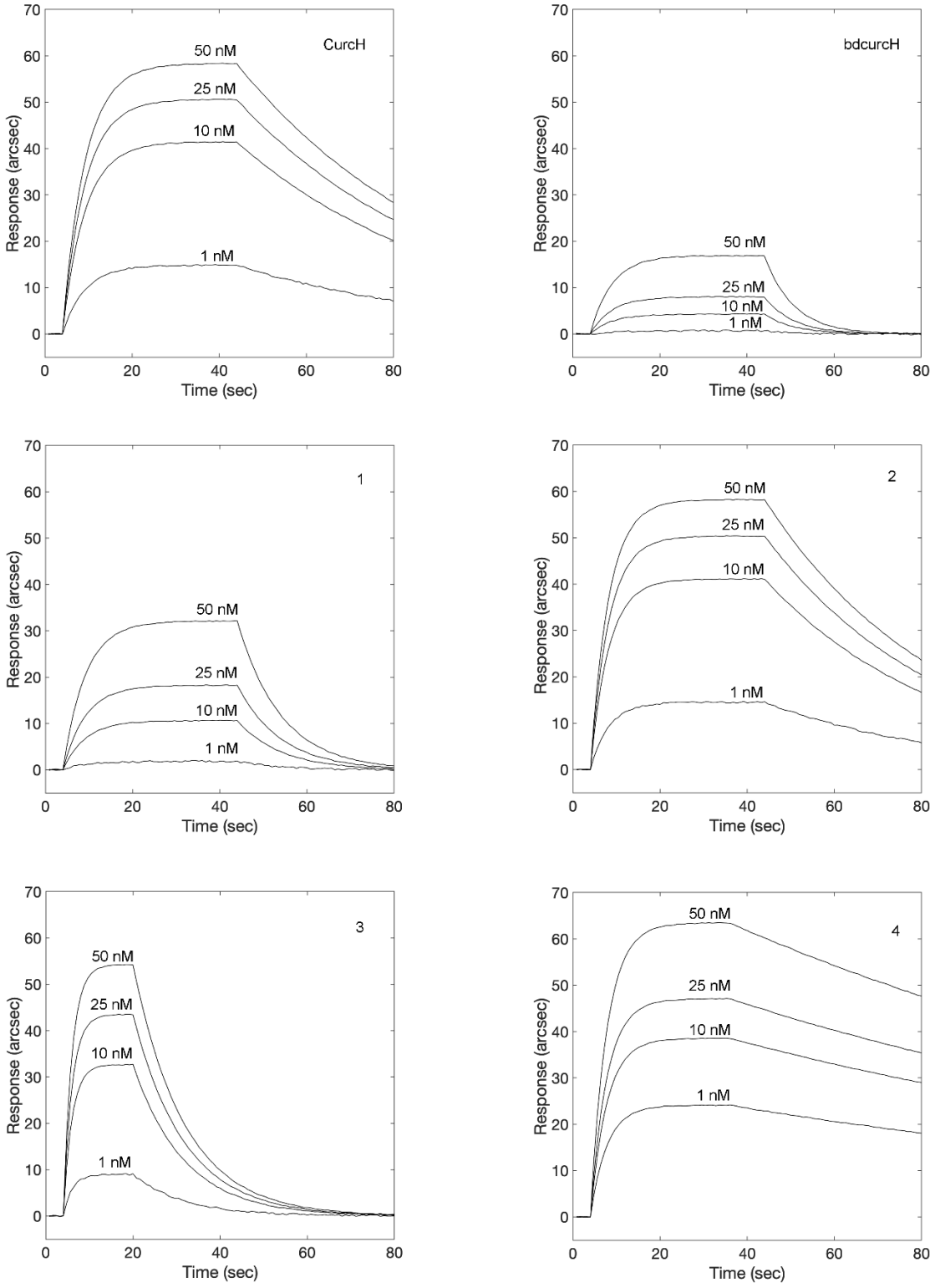

Fig. S56. Superimpositions of mono-exponential binding curves obtained upon independent additions of different concentrations of curcH, bdcurcH and compounds **1**-**4** to surface blocked HMGR.